IMPROVING SPORTS VISION DIAGNOSTICS USING

WIRELESS ELECTRO-OCULOGRAPHY

SUPERVISED BY: Professor J. Tapson
Department of Electrical Engineering
University of Cape Town

PREPARED BY: Dominic A. Wills
Msc (Eng) Student
Department of Electrical Engineering
University of Cape Town

29 September 2006

ACKNOWLEDGEMENTS

I would like to thank the following people:

To Professor Tapson, for his calm manner, inspiration, wisdom and guidance in supervising and funding this project.

To Sam Ginsberg, for assistance in Printed Circuit Design and Microcontroller Advice.

To Rhomco, for their friendly advice and offering their soldering service free of charge.

To Kate Grant and Jo Hotchkiss, for their work in the field of EOG and Zigbee Wireless Data Transmission.

To Robyn Verrinder, for expert advice and assistance.

To Tim, for always supporting my pursuits in academia.

To my brothers Ollie and Andy for their support and good company.

To Peta, for always listening even when I make no sense.

And finally,

To my Mother, for providing massive support to me throughout all of my recent endeavours within academia and extra mural.

DECLARATION

I declare that the contents of this paper are entirely my own work. All external information that has been obtained has been clearly referenced.

signature removed

Dominic A. Wills **29 September 2006**

TERMS OF REFERENCE

This thesis was commissioned in June 2005 by Professor Tapson for the fulfilment of a Master's Degree in Science in Engineering.

This thesis investigates the use of Electro-Oculography in detecting eye movement for the benefit of sports vision applications. It is intended that the work would cover ground work in the field of EOG including:

- The origin of the signal
- Investigation into how to record the EOG signal
- Implementation of the electronics to capture the EOG signal
- Suitability of the signal for adaptation of EOG to a sports application
- Including a wireless platform to transmit the EOG signal
- Design a suitable method of housing EOG electrodes to maximise comfort
- Build a suitable facility to test the hardware

Visual awareness and acuity is a top priority in training high performance sportspeople, however, the results of this training are mostly evaluated in how players feel they are improving. The system objective was to provide a hardware diagnostic solution to a problem in sports vision that there is little available in order to verify the effect of coaching methods and techniques.

This hardware was designed to be used in conjunction with sports coaches in order to be able to perform tests on sportspeople in order to:

- Highlight their visual strengths and weaknesses
- Record improvements in their visual ability over a period of time
- Provide a method for coaches to investigate the results of different training techniques

This is a cross disciplinary project that was seeking to create a unique solution in combining electrical engineering and sports vision.

SYNOPSIS

Introduction

In the fast developing field of sports technology, sports vision is currently receiving much attention as it is recognised as an underdeveloped area of sports research in which vast improvements can still be made. In making improvements in this area, coaches have developed advanced techniques in order to increase visual awareness and acuity. However, the methods that are used for testing still have room for improvement.

Traditional techniques such as eye hand coordination tests have difficulty isolating the pure eye movement data as their results are reliant on subjects performing physical responses to visual stimuli. What is needed in this field is diagnostic equipment that can give information on eye motion alone.

Electro-Oculography was investigated as a form of eye tracking as it is an inexpensive, simple, underdeveloped and primary method of eye tracking that required low data transmission rates. It is flexible enough to be able to fit into a pair of goggles and poses little hindrance to a subject while testing.

Literature Review

The object of this cross disciplinary investigation is to introduce Electro-Oculography into Sports Vision. In order to achieve this, it is important to investigate each research avenue.

The human vision system is limited in that is can only process visual information with 100% visual acuity within 3° of its frame of view. This phenomenon is due to large numbers of the high definition cone tissue located in the centre of the retina (fovea) whose density tapers off very rapidly as we move into the area of

peripheral vision. Our weak peripheral vision causes the eye's movement strategy to behave as a series of *fixations* and *saccades* which takes samples of our visual scene and uses these samples to create a map of our peripheral vision. In this study, we are interested in the saccade parameter as this contains the eye movement information.

Two methods of eye tracking were investigated. Infrared eye tracking makes use of the property that the retina is a very good reflector of infrared light wavelengths. Infrared light shines from an LED and uses a small camera to detect the retro reflected light. The video is analysed using imaging techniques and the pupil position is plotted.

The eye can be modelled electrically as a dipole as the cornea is positively charged relative to the retina. Electro-Oculography uses this corneoretinal potential of the eye to interpret changes in electric field in the outer canthi as eye movement. This is a biological signal and is subject to interference and DC signal drift caused by changes in skin potential.

The Sports Vision EOG System

The overall EOG system design is made up of five components.

1. The electrode system houses the electrodes and is responsible for the primary pickup of the EOG signal and transmitting this signal to the EOG circuitry.
2. The EOG interpretation and transmitter circuit board is responsible for amplifying, filtering, digitising the EOG and transmitting it wirelessly.
3. The EOG receiver circuit board collects the EOG information and controls the visual test facility allowing it to combine the stimulus and response data information in one packet.

4. The visual test facility provides a frame of independently programmable illuminating LEDs which provide the stimuli for testing.
5. The PC is responsible for post processing the data and calibration.

The Electro-Oculogram

Implementing the capture of the electro-oculogram requires placing silver/silver chloride electrodes in positions around the eye that are orthogonal to their axes of rotation. This gives the ideal EOG signal free of any channel crosstalk, however in most cases the ideal scenario is not possible and thus a linear transformation can be applied to the channels to correct undesirable crosstalk.

A pair of electrodes is connected to the inputs of an instrumentation amplifier which performs a subtraction of the two signals. The result of this calculation is the electro-oculogram. The signal is then filtered and a series of adjustable summing operational amplifiers is used to add a DC signal to the EOG signal in order to neutralise the undesirable effect of DC drift.

The geometric positioning of the electrodes and their position relative to the rotating eye dipole, in conjunction with the electrode physics gives rise to a non-linear relationship between gaze angle and electrode potential. The relationship can be assumed to be linear for gaze angles less than 30°.

EOG Circuit Design and Construction

The EOG capture circuit board was required to be small and discreet as it had to be mounted onto a pair of goggles. A printed circuit design most suited the project as it met the space requirements and allowed us to use the Freescale MC13192 wireless transceiver which is a surface mount component. The board was made up of three main components:

1. EOG signal capture and filtering and manual neutralisation of DC drift.
2. Microprocessor circuitry with serial transmission to wireless transceiver.
3. Wireless Circuitry with printed antenna and crystal oscillator.

Microprocessor Use and Programming

There were two microprocessors used in this project, both from the MC9S08GTXX family. They were used at the heart of all data transfer which included A/D conversion of analog signals, SPI connection with the wireless transceivers, parallel transmission to the visual test facility and SCI connection to the PC. Other features that were used included the timer channels. The microprocessors were programmed in C and assembler using Metrowerks and the SMAC.

Zigbee Wireless Data Transfer and SMAC

The 2.4 GHz Freescale MC13192 wireless transceiver was used due to its small size, low power, high data rate and ease of use. It is capable of transmitting at 250 kbps whereas this application only required 6.44 kbps. It is also designed to work in tandem with the family of processors which was used in this project. The operating range was 10m line of sight.

The simple media access controller (SMAC) is a software package released by Freescale in order to help developers of wireless applications. It contains the stack of code needed to control the MC13192. This was used as the basis for developing the wireless platform needed to transmit the EOG signal.

The Visual Test Facility

The visual test facility is a critical part of the project as this provides the input stimuli which is compared with the output EOG data. The facility was mostly concerned with performing saccadic eye movement tests (SEMT) as this suited the application and the EOG hardware.

Eight red LEDs are sunk into a black frame and are independently programmable in both timing and sequence, they can also be programmed to illuminate in a random sequence. The test subject is required to follow the test pattern with their eyes while the EOG unit logs the eye movement data. The LEDs are controlled by the same unit that receives the EOG data. This allows the unit to packet the input and output information together.

High Level Software

The software used to receive and process the EOG data begins with Visual Basic Program that receives the serial data and writes it into a text file. This text file is then imported into Matlab.

We use Matlab for the filtering and calibration of the EOG, timing and LED data. This process converts the 5 bit data packet of Horizontal and Vertical EOG (2 bits), Timing Registers (2 bits) and the LED information (1 bit) into real world variables that can be graphically interpreted. This also includes removing the DC drift from the EOG signal.

Results

The EOG goggles proved to be comfortable and non-inhibitive but possibly not versatile enough to fit small faces. The initial instrumentation and filtering of the EOG signal worked well, however the manually adjustable DC drift neutralisation

didn't provide enough online control. The microprocessor and wireless transmitter performed as required. The EOG test results proved to be very useful as we were able to get accurate readings in a SEMT for saccadic latency, peak velocity and overshoot. The sample rate was 140 samples per second.

Conclusions and Recommendations

The overall system completed its objective as we received data that was in line with tests completed in other publications. The system is however, still subject to improvement. The EOG electrodes could be mounted into a more discreet pair of eyewear which would allow for even more flexibility and the DC drift reduction would be better controlled as an online feedback loop. The test results are compared to the SEMT tests in [25] which showed comparable results in saccadic latency and peak velocity.

I would recommend that this project is investigated further. A full EOG and dark testing room could to be set up containing the visual stimuli hardware and the EOG. A subject would be placed in a chair and be subject to a full test in controlled conditions. This would add to the consistency of the test so that different subjects could be compared. The analysis software could also be upgraded so that a program could be run to extract the eye performance parameters that we want. This would enable us to produce results soon after testing in order to give quick feedback.

TABLE OF CONTENTS

TABLE OF FIGURES

1 INTRODUCTION

1.1 Background to Study

Current sports research casts an ever-expanding net around a vast variety of factors that are believed to be capable of increasing an athlete's performance. We are striving to make fine improvements that result in fractional increments which within the closeness of today's competition could provide crucial match winning advantages. This is visible across the spectrum, as each sport is constantly looking out for a new coaching method or training technique that can give them a unique advantage.

One area of sports research that has recently started to show promise is the area of sports vision. Sports vision has always been highly regarded in deciding the ability of a player. A high visual acuity and the ability to move the eyes quickly has been the cornerstone of high performance sport for decades. Interestingly though, until recently, eye performance has never actually been isolated from the hand and brain functions.

Experts have traditionally been interested in eye-hand coordination. There are various tests designed to analyse this. Subjects are required to press various buttons on an apparatus depending on various visual stimuli. This gives the assessor an indication of a player's ability to complete a particular chain of eye hand coordination events. This chain might look like the following:

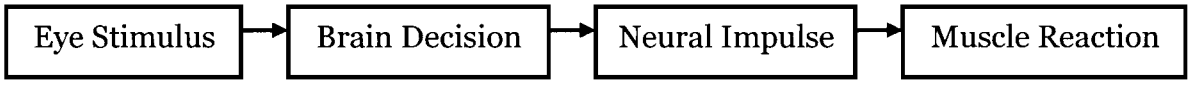

As can be seen from the block diagram above, the eye hand coordination gives a timing indication about four faculties working in unison. The eye is the first receptor of the signal, which is then transferred to the brain through the optic

nerve where a mental decision is then made about what response to make. This response is actuated through a motor neural impulse.

Each stage in the above chain of events has an inherent time delay included with its process. The eye takes some time to receive the signal and convert it to a neural signal, the neural signal takes time to be transmitted to the brain, the brain takes some time to make a decision and the motor neural impulse takes time to cause a physical reaction.

The eye-hand coordination test gives an accurate indication of an athlete's ability to complete an overall eye hand movement task, and modern timing sophistication can be used to rank an athlete in various categories according to his time response to the various tasks.

Looking ahead, the next step is to isolate each step and ascertain how much time each step in the chain takes to complete. If we took two players with identical eye-hand reaction times, further analysis might show that the majority of their time is spent performing different tasks. An example of this might be two cricketers; one player might have above average eye-brain coordination with below average motor neural capabilities, while the other player might exhibit a below average eye-brain performance capacity with an above average motor neural ability. These players would exhibit similar eye-hand performance characteristics, despite differences in the makeup of their internal eye-hand coordination routine.

Modern coaching and training techniques have identified different methods in training these two players and for this reason it is vital for a test to be developed that can draw a distinction between the two. There is a demand for technology that can isolate any of the steps in the chain reaction that defines eye-hand performance.

1.2 Problem Description

The challenge at hand is to investigate a method that could give accurate eye movement parameters that would be useful for a vision coach. It would need to be able to ascertain all of the eye performance characteristics of a player. This information would include eye reaction time, eye movement speed, eye movement non-linearities and oculomotor control parameters such as overshoot.

This method would have to be practical. It would have to be designed so that a sportsperson could wear it comfortably and not provide any visual hindrance during testing while maintaining a high level of timing and eye movement accuracy.

1.3 Objectives and System Description

In order to assemble a system that could respond to the demands of the criteria listed in section 1.2, one particular solution seemed to provide a good avenue to investigate. This method was Electro-Oculography. It seemed a good method for various reasons:

- It was an underdeveloped method of detecting eye movement within the field of sports vision and thus provided lots of scope for research.
- It was an easy and cost effective method to investigate as no major hardware was required to set up a small testing facility.
- It seemed to be the least inhibitive method to use, having the potential to have no discernable effect on the integrity of the collected data.
- It could be mounted onto a pair of goggles which are light and easy to wear.

- Low data rate requirements meant that it was simple to integrate the system with a wireless platform over which to send data. Eliminating the need for conducting wires added to the user friendliness of the system.

The electro-oculogram system used in this project comprised a set of electrodes which were mounted within the frame of a pair of goggles in the exact positions that gave the most accurate eye movement data. These electrodes were then connected to instrumentation circuitry on a printed circuit board. The signal generated by the electrodes was then amplified, filtered, digitised and communicated over a wireless link to a nearby receiver board. This receiver board was primarily concerned with receiving the data and transferring it to software loaded on a computer over a serial link.

The data would then be received by a Matlab program which contains some programming designed to extract the desired performance information from the raw data. This performance data is the final product that would be available for analysis by the relevant visual performance coaches.

1.4 Scope and Limitations

The project concerns itself with combining the disciplines of electrical engineering and sports vision. In an interdisciplinary project such as this, one would like to have an equal opportunity for development in each field. This did not turn out to be a practical reality as contacts within sports vision were difficult to track. This caused the project to be more electrically biased as the scope for testing in the arena of sports vision was limited.

On the electrical side, there was a lot of scope for development into printed circuit design, different options for wireless components and electrode housing. This directed the project more along the route of developing good EOG technology, and leaving the sports vision application for a future project.

1.5 Plan of Development

This development of the text begins in chapter two with a literature review of areas of interest in both disciplines. A description in chapter three of the entire system is then included in order to familiarise the reader with the different aspects of the project. In chapter four, we take a comprehensive view of all aspects of Electro-Oculography from the origin of the signal to the electronics needed to implement it. The electronic implementation is continued in chapter five where we discuss the printed circuit design and construction. We then develop the microcontroller and wireless units along with the programming of each in chapters six and seven.

Chapter eight discusses the visual testing facility and the various testing processes that are performed. Chapter nine then discusses the high level programming used to complete the testing process to evaluate the final diagnostics.

We then move towards the results in chapter ten of how the application design worked, evaluating each design stage and looking at the complete package. The conclusions in chapter eleven compares our results with the results of other studies to decide whether the results are consistent with previous work and chapter twelve discusses some recommendations by the author for future work in the field.

2 LITERATURE REVIEW

The significance of this project is twofold. It is a cross-disciplinary design and therefore tries to marry the technological developments in eye tracking and use them in such a way as to benefit researchers in the field of sports vision. This project was not concerned with investigating much further into eye tracking than has previously been achieved, but it is using eye tracking in a field where it has not yet been used. Thus the design challenges were concerned with using previously existing technology and adapting it so that further advances can be made in the research field of sports vision.

The following section contains an overview of all of the information that has been gathered in the field of vision for the purposes of this study. This section will include information about the eye and how it operates in addition to notes on the movement strategy of the human vision system.

2.1 Introduction to Human Vision

This section is designed to help the reader understand how the eye works and how this makes our visual system behave.

2.1.1 The fovea

The retina of the eye is made up of millions of photoreceptors. Their job is to convert the light that is focused onto them into neural signals that can be transmitted along the optic nerve to the brain. The diagram below shows the two main types of photoreceptors; these are rods (blue) and cones (red).

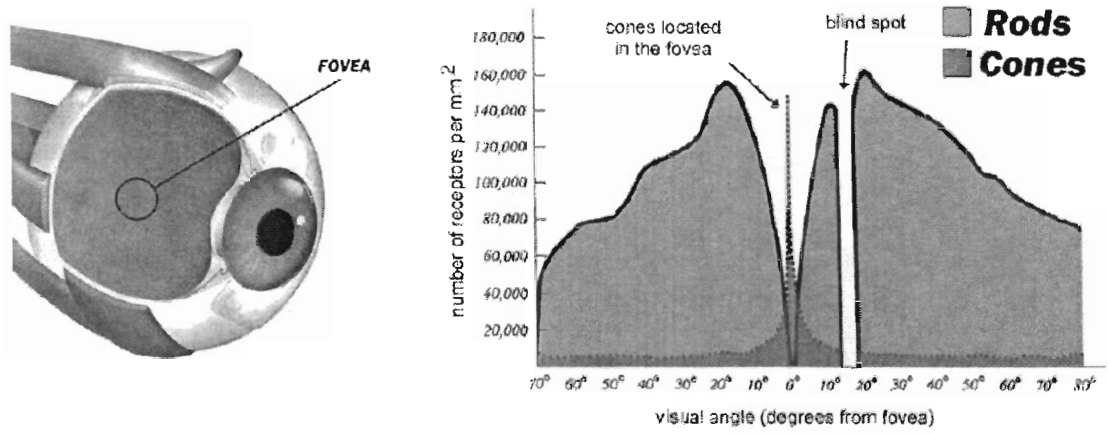

Figure 2.1: A depiction of the spatial distribution of the rod and cone type photoreceptors [11].

The rod photoreceptors highly outnumber the cone receptors and are largely responsible for vision in low light conditions such as at dusk and dawn. Figure 2.1 shows us that the rods are highly concentrated outside the centre 5° of visual angle, which marks what is commonly known as peripheral vision. The rods' poor recording of colour and resolution results in a low definition human peripheral vision system.

The cone photoreceptors are a high resolution, high colour receptor and are most densely concentrated in the optical centre of the eye. They are connected to an almost direct neural path to the visual cortex and are responsible for controlling the major portion of the neural tissue in the brain. This high density area of cones is called the fovea and gives 100% acuity for the light that is focused on it. Figure 2.1 shows the density of cones falling off very rapidly from the centre of vision which causes a corresponding reduction in visual acuity.

2.1.2 The Human Visual Movement Strategy

This spatial distribution of the two types of photoreceptors makes the human visual system unique in the way that we only have 100% visual acuity in 3° of our frame of vision [29]. Consequently, we have to actively take many visual samples

of our surroundings in order to map our periphery. This process of looking around includes employing a series of *fixations* and *saccades*.

2.1.2.1 Fixations

A *fixation* is a point on which the oculomotor control system is focused on. In order to perform a fixation, the eye has to control the lens, the pupil and the eyeball in such a way that the object that is being fixated lands fully focused on the fovea of the retina. This can be thought of as the brain taking a sample.

2.1.2.2 Saccades

A *saccade* is the rapid eye motion that moves the eye from one fixation point to another. During a saccadic eye movement the peripheral vision sends a signal to the brain highlighting a target, which in turn activates the oculomotor control system to effect the appropriate eye action. The eye then moves rapidly toward the object and upon landing on it, it slows down and fixates itself on the target. Saccadic Eye speeds can exceed 700°/s.

It is through this series of fixations and saccades that the human oculomotor system operates. As the eye traverses a scene, it does not move in a smooth motion, it locks onto mini targets along the way, fixating on each before saccadically moving on. At each target, the visual information is registered in the brain and stored to help create complete scene vision.

The next part of the literature review involves looking at different methods of eye tracking. The two forms of eye tracking that were investigated in this study are described in the following sections.

2.2 Infrared Eye Tracking

Infrared Eye Tracking has crossed many application barriers in the last five years. It has moved from being a mostly laboratory-based tool, to one that can be used outdoors in a variety of ways. At the Rochester Institute of Technology, researchers have been working on making a portable infrared and camera based eye tracker and have published a practical article on how to build one [10]. This initiative is aimed to encourage an open source type of development of this technology.

2.2.1 Theory of Infrared Eye Tracking Operation

One method of infrared based eye tracking makes use of a tracking technique called ***bright pupil illumination*** in combination with an infrared based video detector [11]. This method uses the fact that the retina is very reflective (while not sensitive) of infrared light wavelengths. This phenomenon is often exhibited in photographs of people where a "red eye" effect is commonly observed. Due to the retina being a diffuse, retro reflector, long wavelength light from the flash reflects off the retina and upon exit back illuminates the pupil. This property gives the retina a reddish cast [12].

Bright pupil illumination eye tracking uses an infrared source of light which is shined onto the eye from a close distance. Due to the infrared reflective properties of the retina, there is a strong reflection from the retina which shines through the pupil, while a weak signal is received from other parts of the eye scene. The light reflection is detected by a camera with an infrared filter placed over the lens. This produces a picture of the eye with the pupil highlighted. An example of what this reflection might look like is shown overleaf:

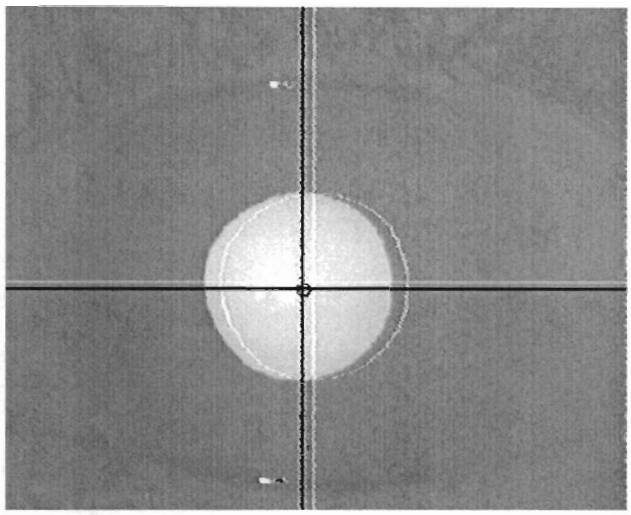

Figure 2.2: A view of the eye through an infrared filtered camera lens showing the reflection from the retina through the pupil [12].

If you look closely at figure 2.2, you will see that there are two small reflections above and below the eye. These are called Purkinje reflections and they are generated as the first surface corneal reflections. It is the difference between this reflections and the centre of the pupil that generates the vector necessary to compute the angle of pupil rotation.

In the following diagram, the angle of rotation is calculated from the pupil-corneal reflection separation by:

$$PCR = k\sin\theta \tag{2.1}$$

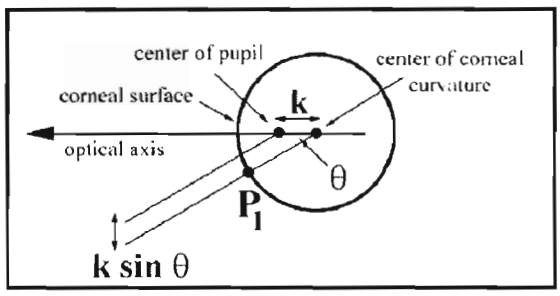

Figure 2.3: This diagram depicts the eye and describes the relationship between the angle of rotation and the pupil corneal reflection [10].

Another method of implementing infrared eye tracking is by using a technique called ***dark pupil illumination.*** It makes use of the same principles used in *bright pupil illumination,* except that it uses an IR LED that is off axis with respect to the camera's focal axis [10]. In this setup, the infrared reflection from the retina is not seen by the camera and therefore leaves a dark area where the pupil is. This can be seen in figure 2.4. This technique makes use of the equation 2.1 as used in *bright pupil illumination,* which makes use of the first Purkinje reflection.

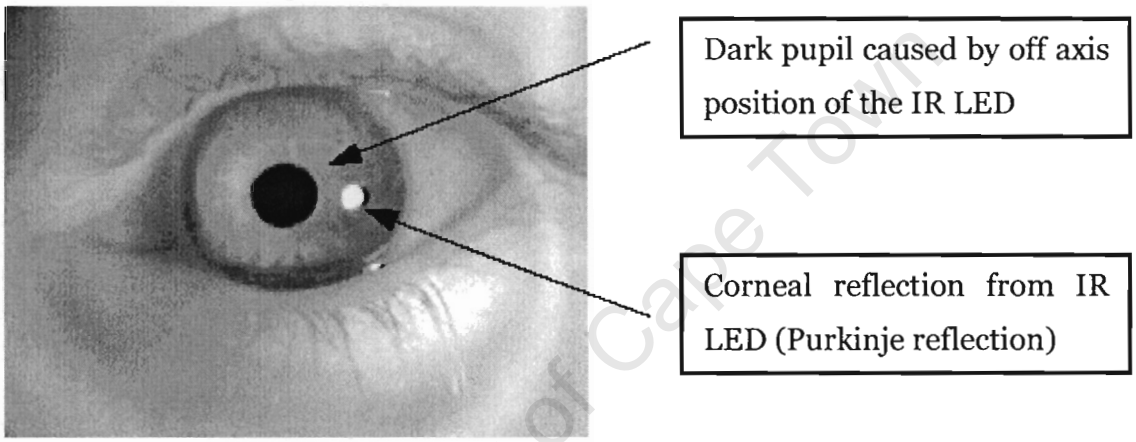

Figure 2.4: This diagram depicts the dark pupil illumination technique [10].

All of the methods described in this section are combined with an outward pointing scene camera which provides the exact scene view that the eye has. When these systems are combined and correctly calibrated, you can produce a video of what a subject sees with the exact location of their eyes in the view.

2.2.2 Infrared Eye Tracking Hardware

The hardware equipment required to implement IR Camera Eye tracking is divided up into two sections:

- The physical hardware and head unit used to ascertain the eye position and scene views

- Image processing software and the bulk storage

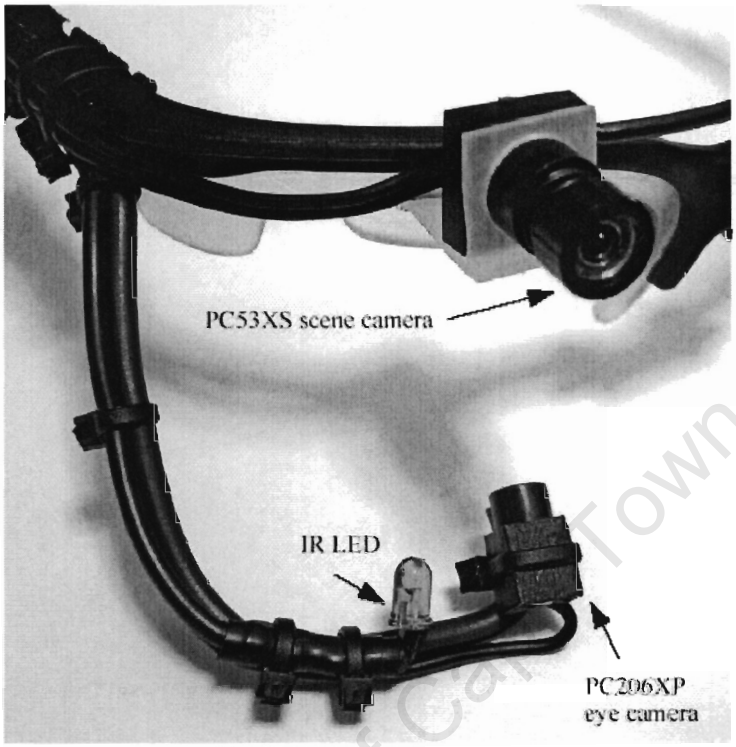

Figure 2.5: A diagram displaying the IR Eye tracking headgear equipment [10].

Figure 2.5 shows the scene camera mounted at the top of the eyewear frame. Near the bottom of the picture we can see the IR LED and the Infrared Detection Camera both pointing to where the eye would be. The *dark pupil illumination* technique is used in this case which makes the construction easier as no IR-pupil alignment has to take place.

The above apparatus is connected to a portable computer and battery pack. The purpose of this is to run the image processing software and to be able to output and store a video of the subject's scene view superimposed with the cross showing the exact location of the eye.

2.3 Electro-Oculography

Electro-Oculography has been an existing technology for long enough that the advantages and disadvantages are widely known. Technical solutions to the difficulties of implementing EOG are also well documented. However, each different application of EOG gives rise to new challenges which need to be overcome.

2.3.1 Introduction to EOG

Emil du Bois-Reymond (1848) first observed that the eye's cornea is positively charged relative to the retina [1]. At the time, this static potential was thought to be independent of light, but since then it has been shown to exhibit time varying characteristics.

Electrically, the eye can therefore be thought of as a solitary dipole rotating within a confined 3-D space (eye socket). The size of this corneoretinal potential is usually in the range of 0.4-1.0 mV [1]. As the potential rotates within the eye socket, it creates a dynamic potential which is sensed by the electrodes, and eye rotation data can then be extrapolated. This extrapolation is called the Electro-Oculogram.

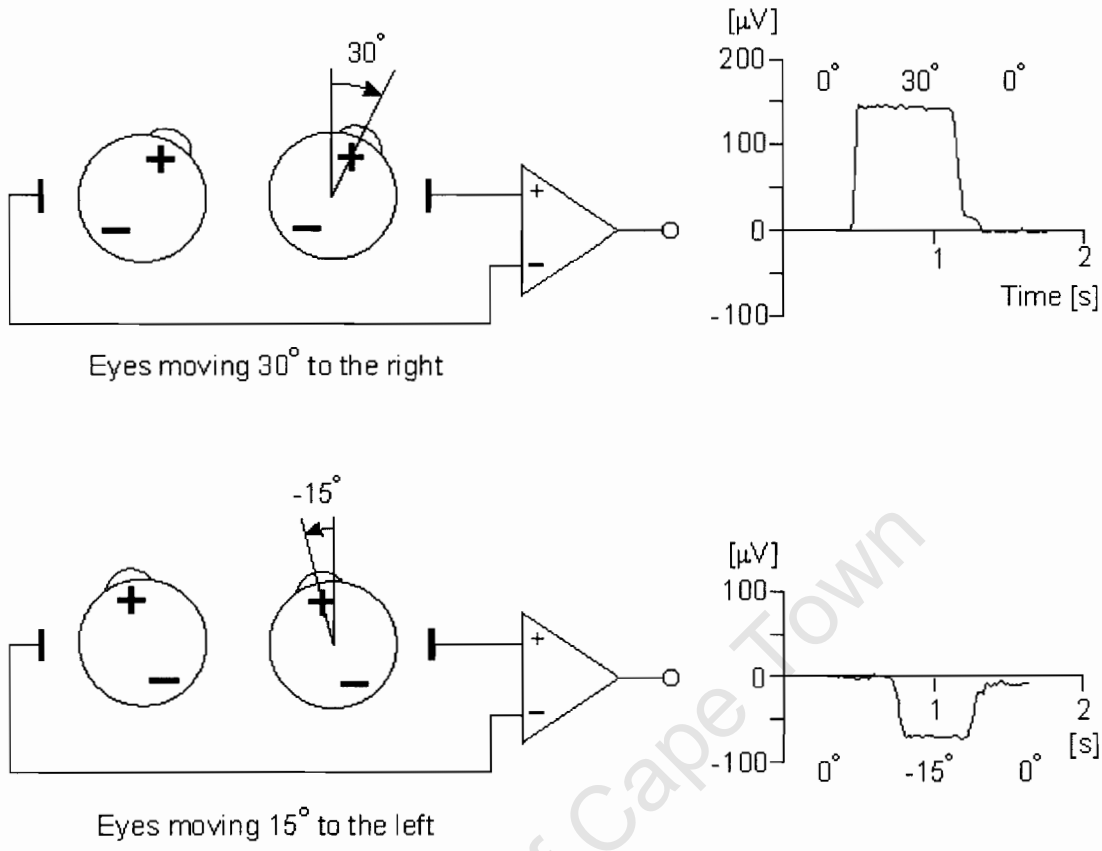

Figure 2.6: This diagram depicts electrically how the EOG signal works with horizontal eye movement [1].

Figure 2.6 illustrates how the EOG signal is recorded. In the first diagram, the eye moves 30° to the right. The potential difference is measured by a pair of electrodes connected to the positive and negative terminals of an instrumentation amplifier. This instrumentation amplifier subtracts the signals and outputs the result of this calculation.

The known accuracy of the EOG is between 1° and 3°, with a maximum rotation of 70°, however the signal becomes non-linear for angles beyond 30° [2]. The size range of potentials one can expect to receive from EOG electrodes are between 5 and 25 μV/°.

2.3.2 Advantages of EOG

The known advantages of EOG are mostly involved with the fact that the EOG signal is present at all times. This allows for studies in poor lighting situations, as well as tests with the eyes closed. It is also simple to implement and a subject can be tested with relatively minimal discomfort and intrusion.

2.3.3 Disadvantages of EOG

The EOG signal is a constantly varying signal according to light, fatigue and other qualities [1]. Thus, it is possible to have your eyes fixed on a certain position, and detect a slowly changing EOG signal. This makes the signal difficult to calibrate directly and calls for some signal conditioning.

2.3.4 Eradicating Slow Potential DC Drift

The EOG is a biological signal and is subject to various sources of noise. These noise signals could be made up from brain activity, changes in surface skin resistance and muscular activity. These noise signals can be filtered out to a large extent, which renders them controllable, but there is another signal present that presents a bigger problem. This problem is a DC signal that lies in a similar frequency band to the EOG signal and is therefore difficult to filter out.

The slow moving DC Drift is the most documented issue with implementing EOG hardware. The problem is described as a time variant DC potential that underlies the signal generated by moving the eyes. Consequently, a 30° gaze angle at time t could generate a differing potential to the same gaze angle at a time $t+n$. This signal discrepancy creates a problem where positional accuracy is of importance eg: an eye controlled computer mouse.

There are three major methods that have been proposed to control the EOG DC Drift.

2.3.4.1 Treating the waveform as Alternating Current

Some applications require only acquiring the transient behaviour of the eye. These applications are concerned with eye speeds and require no positional accuracy. An implementation method for this type of application is suggested in [5]. In this case, the DC value of the EOG signal need not be recognised, therefore the signal can be passed directly through a capacitor and measured on the other side. This will give the changes in the signal only. If positional data is required, some success can be gained by the integration of the signal.

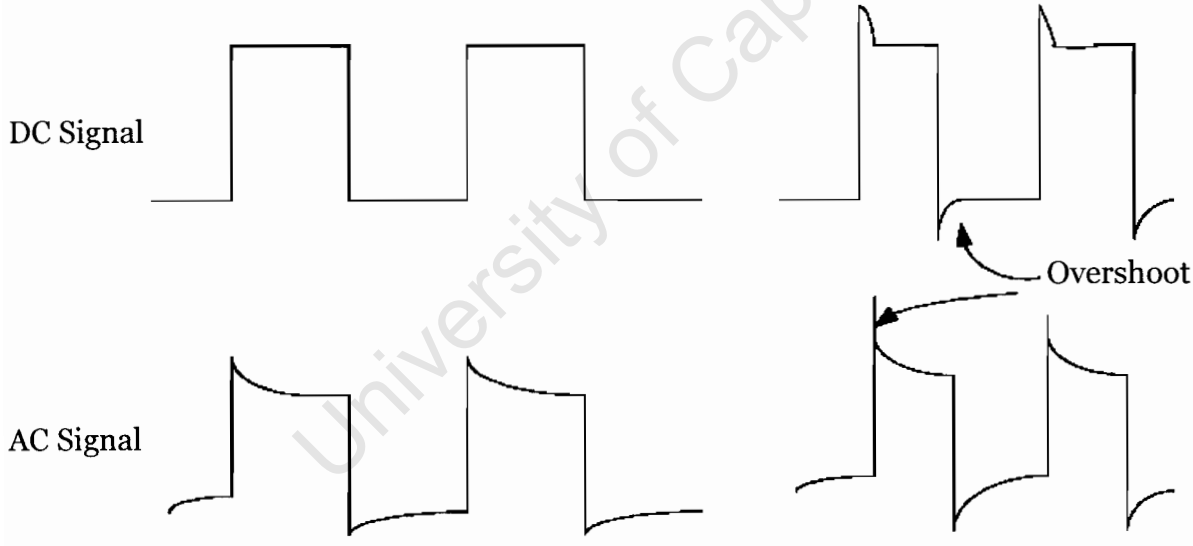

Figure 2.7: The diagram depicts a DC and AC recording during an EOG test [5].

2.3.4.2 Subtracting DC Component from the Signal

The next method of conditioning the EOG signal to remove the drift potential is concerned with separating the signal into two components based on their

frequency. This method is suggested in [5] and the circuit diagram is shown below:

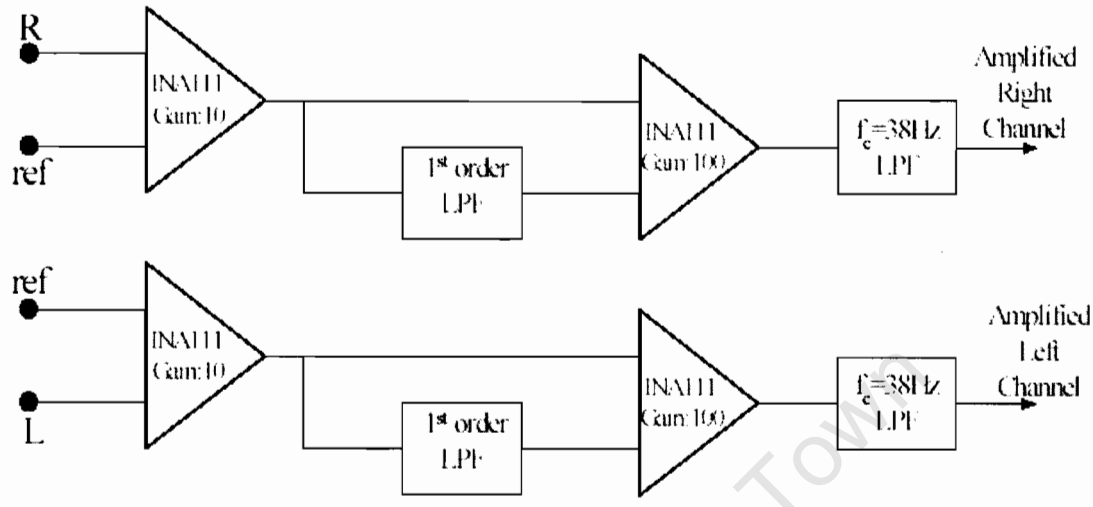

Figure 2.8: This circuit diagram shows the path of the EOG signal being separated and the DC component subtracted from the original signal [5].

The EOG signal is acquired and the initial amplification (INA111) takes place. The next stage involves low pass filtering the signal eradicating all of the dynamic behaviour and leaving just the slow moving DC component. This component is then subtracted in real time from the original signal with another differential amplifier. The result is the original EOG signal without the DC drift.

2.3.4.3 Artificial Neural Networks

In [9], a technique is proposed that uses an ANN to map 2-D eye movement signals into 2D eye positions which can enhance the utility of such recordings. Multi-layer perceptions with non-linear activation functions are shown when combined with back propagation to have improved accuracy of calibration increasing the overall accuracy.

2.3.5 Uses of EOG

The Electro-Oculogram has been used in a wide variety of studies relating to:

- Sleep and REM, EOG is the only suitable method for sleep and blinking applications as it also works when the eyes are closed.
- Schizophrenia research with particular reference to anti saccades, where the subject is asked to look away from a particular stimulus and not towards it [5].
- Disabled person applications including wheel chair guidance [27] and Eye Guided computer controllers.
- Reading studies [28].

3 SPORTS VISION EOG SYSTEM

The purpose of this chapter is to describe the overall system to give the reader a general feel of how this project is put together. The chapter describes the complete design before dividing it up into five main parts and introducing each component separately.

The challenge of the overall system design was to create a device that could realistically be used in ascertaining various visual performance parameters of high performance sportspeople. In order for this to become reality, various general design parameters were stipulated and the solutions for these are outlined in this section.

3.1 Design

The design had to be practical enough so that a realistic test could be set up. The more practical the hardware was, the more realistically the subjects could be tested and the more valuable the output data would be. This practicality dictated that the design would have to be as minimal in size and portable.

It is for this reason that the following design decisions were made:

- The system would have to be easy to set up, calibrate and changing users would require minimal effort.
- Portability and compactness were essential, with a printed circuit design option being preferred.
- Data transfer would be conducted by a low power wireless medium.
- The design had to be low power and battery operated.
- The design had to incorporate a comfortable, robust method of wearing the electrodes.

Taking these considerations into account, a design choice was made which is displayed in figure 3.1.

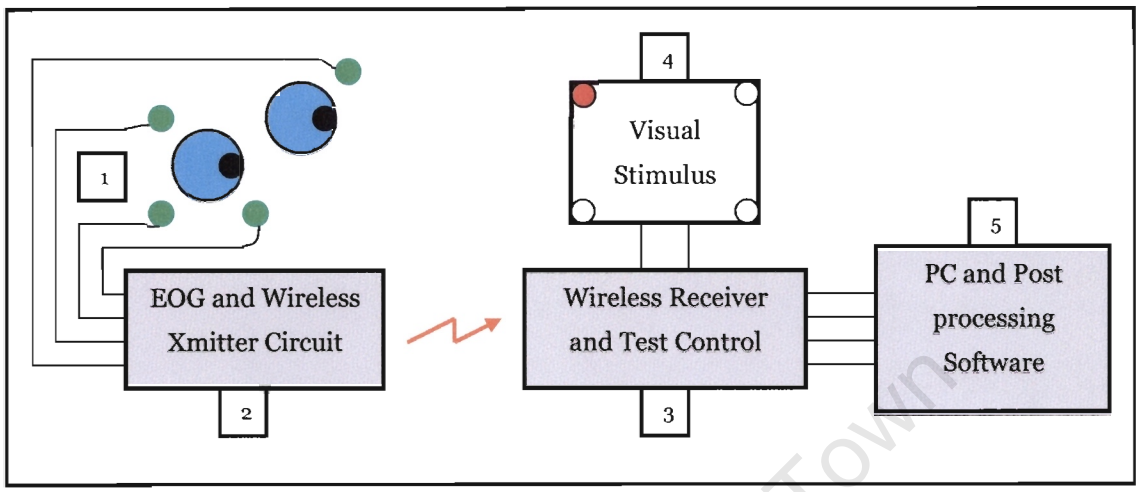

Figure 3.1: Overall System design including EOG electrodes (green), EOG circuit (2), wireless transmit and receive (3), test facility (4) and serial link to PC (5).

Seen in figure 3.1, are five main components that make up the total project design. These five comprise the:

- Electrode housing (goggles)
- EOG circuitry and transmitter circuit board
- Receive circuit board and test facility controller
- Test facility
- PC link and post processing software.

The following sections will contain a version of the above diagram highlighting a specific portion of the project. The section will then give a brief introduction to the purpose of that sector of the project, with more detailed information being available later in the report.

3.2 EOG Goggles

The diagram below highlights the first part of the chain of events that produces the EOG information. It consists of the electrode placement and raw biological signal transfer.

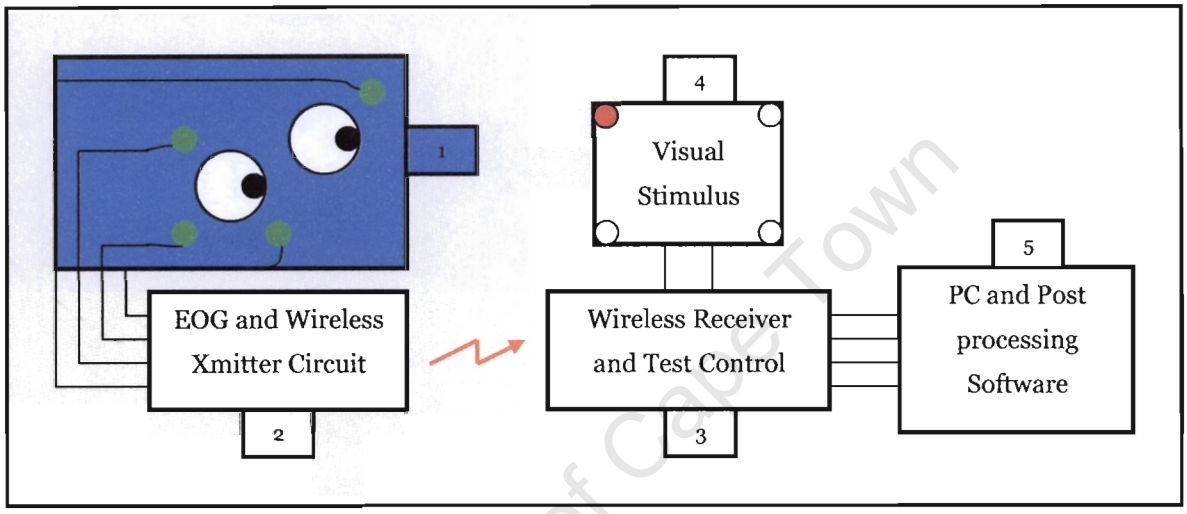

Figure 3.2: System design diagram highlighting the EOG goggles and electrode apparatus

It was agreed that using the basic wired electrodes stuck to the head as used with stationary patients in hospital was not a good design decision for the following reasons:

- The electrode wiring tends to get in the way as the subject moves around. The wires need to be kept neatly away from the subject's face and head during testing.
- The adhesive applied to the electrode to keep it stuck to the skin can become loose and pull away from the skin entirely. It would be better to add extra support.
- There would be no physical support for the wireless EOG transmitting board.

On the basis of the above reasoning, it was decided that some form of electrode housing was necessary in order to boost the robustness of the overall design. Two options were investigated. One was using a scrum cap and the other was using a pair of dirt biking goggles.

It was decided to use a pair of goggles as this provided the necessary support for the electrode that was placed under the eye. The scrum cap only has support above the eye. Despite our design choice, the scrum cap is not an entirely unfeasible option.

3.2.1 Electrode Mounting

Shown in figure 3.3, is the back of a standard disposable electrode as would be attached to the inside of the EOG goggles. The silver attachment on the back of the electrode is a mounting tip which can host a variety of clips. This mounting tip is electrically connected to a gel like substance on the contact side of the electrode which has direct contact with the skin.

Figure 3.3: A 3m disposable skin mount electrode showing the mounting tip on the back.

A clip that was found to be compatible with this electrode is the standard 8mm press stud as used in the linen and bedding industry.

As the electrode is disposable and cannot be permanently mounted onto the EOG goggle frames, it was decided that a mounting clip was to be glued to the inside of the goggles. This allowed the disposable 3m electrodes to be conveniently clipped in and out depending on when the electrodes were to be replaced. The other side of the clip was soldered to an individual wire which provided the conduction path to the electronic circuitry.

3.2.2 Wiring and Board Mounting

The signal wires are run along the frame within the sponge so as to be out of sight and relatively safe from accidental pulling. The wires carry the signals from the electrodes to the left hand side of the subject where there is a circuit board mounted onto the goggle strap. A connector block attaches the signal wires to the transmitter circuit in order to allow the circuit board to be removable.

3.3 Transmitter Board

The diagram below highlights the second main step where the raw biological EOG information is amplified, filtered and transmitted over a wireless link.

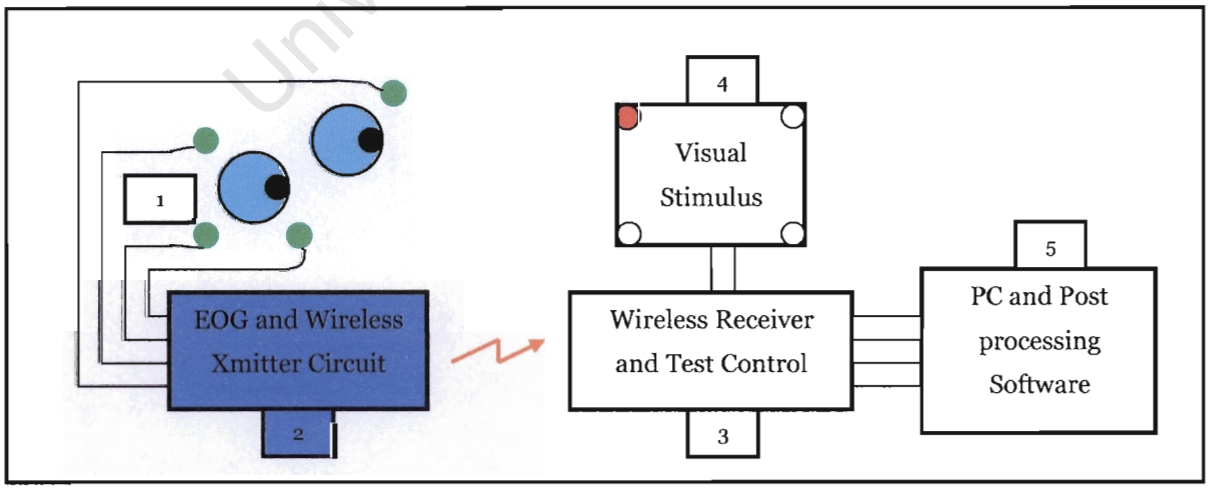

Figure 3.4: System design highlighting the EOG transmitting station.

The transmitter board comprises the EOG signal processing circuitry, the microprocessor and the wireless transfer medium with antenna. The purpose of this board is to:

- Receive the raw EOG biological data from the electrodes mounted around the eyes
- Amplify and filter the EOG data
- Allow for manually configurable range adjustment of the EOG signal
- Convert the analog signal to a digital signal
- Transmit the EOG information over a wireless link to a receiver

The circuit board is battery operated and was constructed using a printed circuit design with surface mount components. This made the circuit small (10x6 cm) and portable. More detail is covered in chapter five on printed circuit design.

3.4 Receiver Board

Figure 3.5 highlights the receiving station which receives the wireless signal from the EOG transmitter. Combined with the visual stimulus information, a packet is created and sent to the PC over the serial communications port.

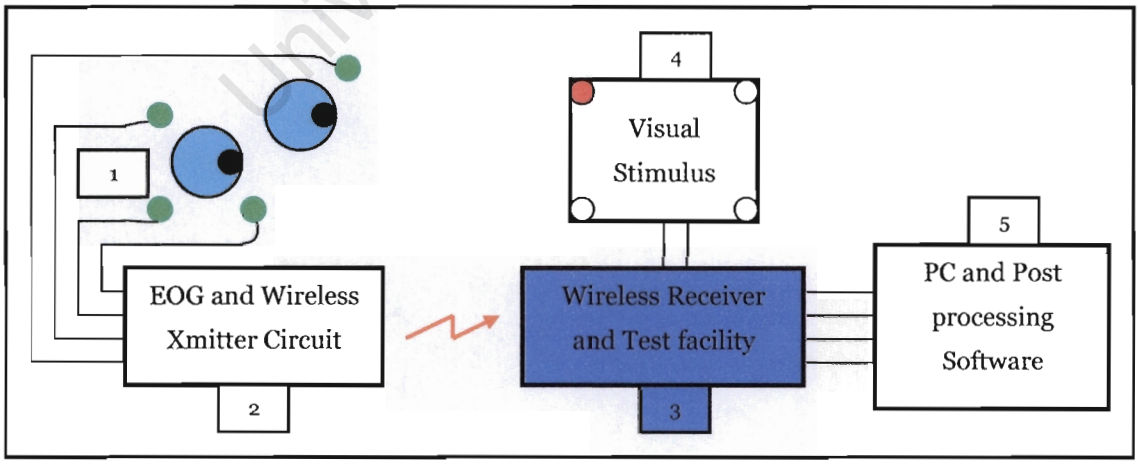

Figure 3.5: Overall System Design highlighting the EOG Receiving Station

The receiver circuit board used was a development kit from Freescale used to demonstrate the Zigbee wireless platform and their MC13192 transceiver. Its functionality includes a serial port interface, three accelerometers, a programming connector which connects to Freescale's BDM Multilink USB programmer, a battery power connector and 12V plug connector.

It includes a Freescale MC908SGT60 microcontroller connected to a Freescale MC13192 2.4GHz Zigbee Transceiver. This combination of components made it possible to receive the wireless signal from the EOG board and transmit it with the stimulus information on a serial path to the PC. The board also incorporates a parallel transmission path which is used to independently trigger the LEDs on the test facility.

3.5 Visual Stimulus Testing Facility

The diagram below shows the test facility which displays a range of individually controlled LED's. This facility can be manually configured to complete a host of different visual tests.

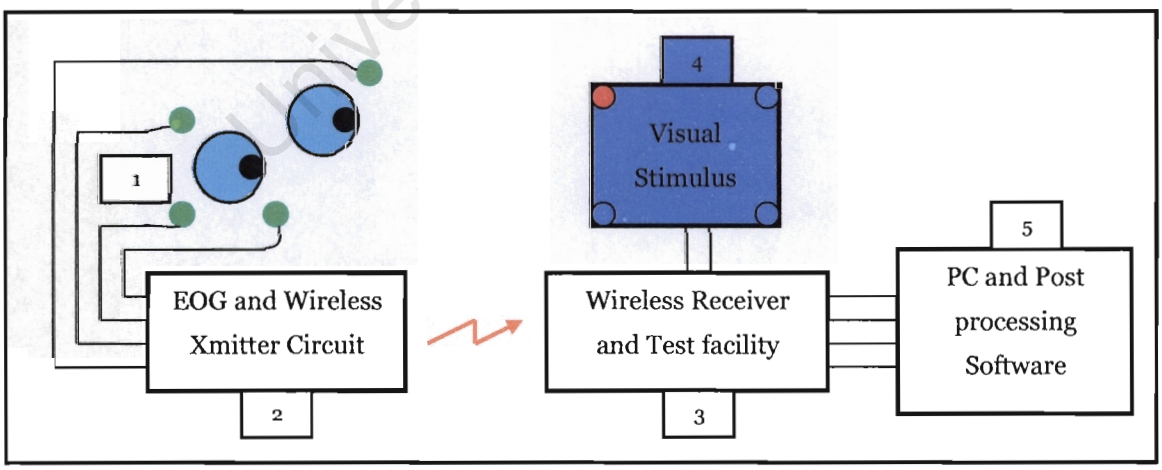

Figure 3.6: The system design highlighting the Visual Test Rig.

The test facility is controlled by the receiver board. It consists of a wooden frame with LEDs sunken into it. These LEDs can be made to flash individually at random or at predetermined intervals to generate a test pattern.

This test output information is combined with the wireless EOG information from the goggles to create a packet containing the visual stimuli and the eye response data.

3.6 Computer Receive Station

The final stage of the EOG data extraction process is shown in the diagram below. In this step, the information is transferred along the serial communication path where the data is received and a range of processing is performed.

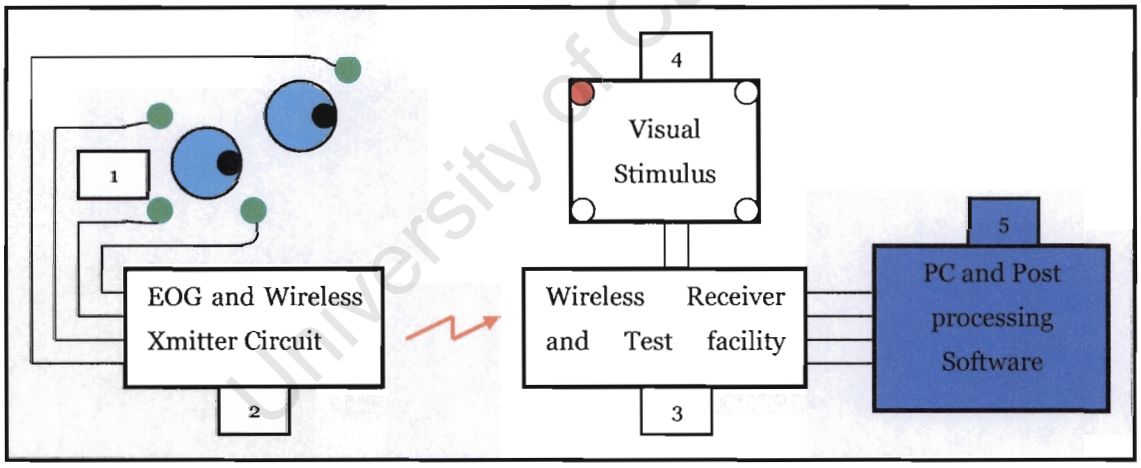

Figure 3.7: The system design highlighting the final stage of data processing.

This part of the project involves all of the post processing of the EOG information that is transmitted.

The computer (PC) station consists of a Visual Basic program that receives the data from the serial port and stores it in a text file. This data is a packet consisting of 5 bytes of information namely horizontal and vertical EOG data,

high and low timer registers and LED illumination information. The program identifies each data string and separates it by a space character.

The next stage of the EOG post processing is concerned with filtering the data, and deciphering it so that it is clean and easy to graphically interpret. This part of the project is carried out using Matlab.

4 THE ELECTRO-OCULOGRAM

An introduction and background to EOG is given in chapter two. This chapter focuses on the electro-oculogram in more detail with particular reference to the current study by looking at electronic implementation, electrode specifications and mathematical modelling.

4.1 Electronic Implementation of EOG

The EOG signal is a biological signal that can be affected by a myriad of external influences such as temperature, light intensity and physical biological properties. It is not always easy to model these external interferences, so the chosen circuit design has to be adjustable to accommodate for them. Compared with other biological signals such as the Electro-Encephalogram (EEG), EOG is quite a large signal with noise interference is relatively low.

The EOG is a static potential and is able to be measured using many of the same techniques as would be used in industrial instrumentation. The modifications needed are mainly concerned with eradicating the DC signal drift. In my design, I opted for an approach where the operator could manually adjust the gain and DC offset. This approach allowed for simplicity and full control of the EOG signal.

The essence of the EOG signal is that it is the difference between the corneo-retinal potentials measured at the outer left and right canthi. The electrodes in contact with these areas are connected to an instrumentation amplifier which takes the difference of the two electrode signals to give a resultant signal proportional to the change in gaze angle.

The electronic circuitry can be divided into three stages as shown below:

These stages are outlined in the following sections.

4.1.1 Instrumentation Amplifier (AD620)

The AD620 is a low cost instrumentation amplifier which requires just one external resistor to control gains of 1-1000 [3]. It was chosen for this EOG application due to:

- Very high accuracy and excellent DC suitability
- Low power required (1.3 mA Max Current[3])
- Low Supply Voltage (±2.3V) and it's suitability for battery operated applications. This application used ±3.3V
- Design allows for a potentiometer to be used to vary the gain
- Available in small surface mount 8 pin package which allowed my circuit design to remain compact
- The AD620 is used in other medical based applications such as blood pressure monitors

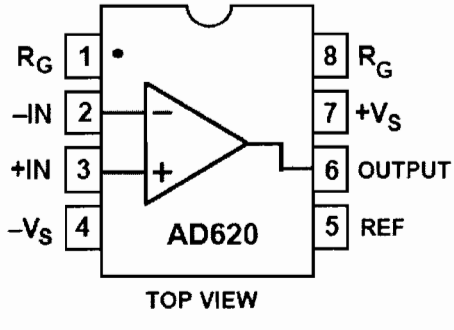

Figure 4.1: Operational Diagram of the Ad620 [3].

4.1.2 Filtering

The human body can be thought of as a signal antenna and can pick up local electromagnetic interferences which can cause a variety of surface potentials to exist on the skin of the human body. These potentials are especially numerous on the head as it is also a source of EEG or "brain waves". For this reason, it is important to isolate the bandwidth of the EOG signal so as to reject the interference imposed by other local signals picked up by the EOG skin electrodes.

The eye moves in saccadic intervals as it traverses across a visual scene. These saccadic intervals are the fastest eye movements possible and vary in speed from 20 - 700°/s. A low pass filter was chosen with a cut-off frequency of 80Hz designed to reject other higher frequency signals while still retaining the integrity of the fastest moving EOG signals.

4.1.3 Adjusting EOG DC Offset

The corneoretinal potential of the two eyes doesn't appear to always be equal, this gives rise to an unpredictable DC offset on the EOG signal which has to be eradicated. It is too small to remove before the instrumentation amplification stage and so it has to be removed afterwards. This DC offset is removed with a summing operational amplifier whose voltage addition is adjustable by a potentiometer. This operational amplifier circuit is also designed with an adjustable gain so as to be able to vary the signal size to meet the A/D converter limits.

4.2 Electrode Selection and Placement

The International Society for Clinical Electrophysiology of Vision (ISCEV) have introduced a set of standards that can be used so that EOG data from different studies can be compared together [4].

4.2.1 Skin Electrode Specifications

In [4], the electrical specifications are given for the skin electrodes. According to these specifications, the following design choices were made.

- Silver/Silver Chloride Electrodes were chosen as they are relatively non-polarisable, and their impedance was not exceeding 10kΩ over the frequency range of 30-200Hz.
- Electrodes placement was preceded by an alcohol based cleansing routine to remove any excess skin oils.
- Disposable electrodes were used for hygienic reasons.

4.2.2 Electrode Placement

In my experiment, I used five electrodes to detect horizontal and vertical movement. Two of the electrodes were placed as close to the left and right canthi to detect horizontal movement, two electrodes were placed above and below the left eye socket and one electrode was placed behind the ear as a grounding electrode. This position minimises cephalic skin potential [7] and is also free from any potentials associated with eye movement.

Another important consideration in electrode placing is the phenomenon of crosstalk, which arises when the electrodes are not exactly in line with the eye's axes of rotation.

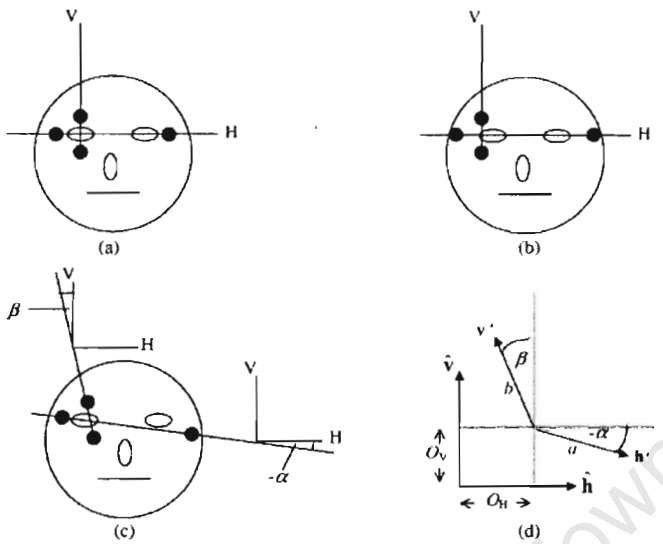

Figure 4.2: Various ways in which inaccurate electrode placement can contribute to crosstalk [9].

Figure 4.2 shows in (a), the ideal electrode placement. In this diagram the electrodes are placed on orthogonal planes, and exactly in line with the axes of rotation of the eye.

In (b), the electrodes detecting vertical eye movement are off centre. While this would not harm the readings for detecting vertical eye movement, a setup like this would add a portion of the horizontal eye movement signal to the vertical eye movement signal.

In (c), we can observe that both the horizontal and vertical movement detection electrodes are improperly placed and in the same way as (b), this will give rise to the signals becoming mixed. This mixing of the signal is the basis for crosstalk.

There is a solution for this given in [9], and it includes applying equation 4.1.

$$\begin{pmatrix} h' \\ v' \end{pmatrix} = \begin{pmatrix} \cos(\alpha) & \sin(\alpha) \\ -\sin(\beta) & \cos(\beta) \end{pmatrix} \begin{pmatrix} a(\mathbf{h} + O_H) \\ b(\mathbf{v} + O_V) \end{pmatrix} \tag{4.1}$$

In this equation, **h'** and **v'** are the readings generated by the horizontal and vertical EOG channels, while **h** and **v** are the actual values. The angles at which the electrodes are off centre are β (vertical) and α (horizontal).

The equation shows a linear transformation matrix that can be applied to correct the electrode placement discrepancy.

4.3 A Mathematical Model of the EOG

It has been previously mentioned that the eye can be described electrically as a dipole. This property is brought about by the corneoretinal potential which is the source of an electric field present about the eye. As the eye moves about within its socket, the fluctuation in electric field is what gives rise to our EOG signal. However, there is little literature that describes the relationship between eye movement in degrees and the bio-potential voltage generated by a local electrode mathematically.

This lack of mathematical documentation was worth investigating, as one of the first and most important considerations in instrumentation is to know what the relationship is between the measured variable and the quantity to be measured. Although in instrumentation, linearity is usually optimal, it is not always necessary. If we know the mathematical relationship between two quantities and this relationship is repeatable, then by using the inverse of the mathematical model to linearize our measurement we can accommodate for the non-linearity in the signal.

It has been mentioned that the accuracy of the EOG measurement becomes non-linear for gaze angles exceeding 30° [2]. No explanation is offered for this phenomenon, so this chapter explores the physical mechanics of the eye and

measurement system to see whether we can offer an explanation for these non-linearities.

4.3.1 The Eye Model

It is mentioned earlier in the chapter that the eye can be represented as a dipole as there is a positive corneoretinal potential that exists creating a potential field. This potential field is measured by electrodes placed at the outer canthi, which measure the skin potentials, the major one being the electro-oculogram.

Figure 4.3 shows a geometric interpretation of the eye that has performed a rotation of θ. This diagram is designed to display all of the significant physical measurements that could be used to model the distance of the electrode from the poles of the eyeball.

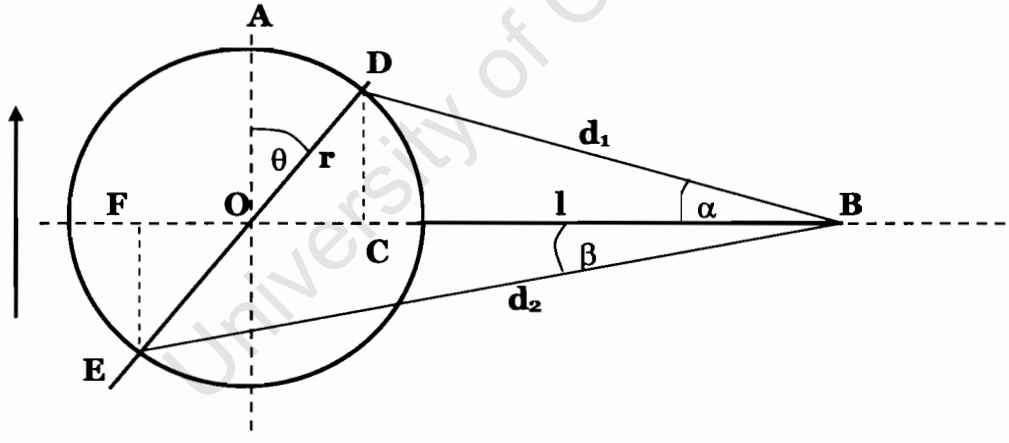

Figure 4.3: A top view of the eye that is rotated θ in a clockwise direction. Also shown is the position of the measuring electrode at B.

The position **D** represents the centre of the cornea; the position **E** represents the centre of the retina. The position **A** is the position of the cornea when the eye is pointed straight ahead. **O** is the centre of the eyeball which can be assumed to be perfectly spherical. **B** is the position of the Electrode. The distances $\mathbf{d_1}$ and $\mathbf{d_2}$ are

the distances between the cornea and the retina to the electrode respectively. θ is the gaze angle, **r** is the radius of the eyeball and **l** is the length BC.

We would like to be able to express the distances $\mathbf{d_1}$ and $\mathbf{d_2}$ as functions of the gaze angle θ, so as to be able to compute the potential at the electrode.

If we look at triangles **AOB** and **DCB,**

$$\frac{AO}{OB} = \frac{DC}{CB} = \frac{r\cos\theta}{l + r(1 - \sin\theta)} = \tan\alpha \tag{4.2}$$

Thus, it follows that

$$\alpha = \tan^{-1}\left(\frac{r\cos\theta}{l + r(1 - \sin\theta)}\right) \tag{4.3}$$

Also,

$$\frac{GO}{OB} = \frac{EF}{FB} = \frac{r\cos\theta}{l + r(1 + \sin\theta)} = \tan\beta \tag{4.4}$$

Thus, it follows that

$$\beta = \tan^{-1}\left(\frac{r\cos\theta}{l + r(1 + \sin\theta)}\right) \tag{4.5}$$

In triangle **ODB**,

$$d_1 = DB = \frac{r\cos\theta}{\sin\alpha} \quad \text{(Sine rule)} \tag{4.6}$$

Using the same methods in triangle **FEB,**

$$d_2 = EB = \frac{r\cos\theta}{\sin\beta} \quad \text{(Sine rule)} \tag{4.7}$$

The above equations give us enough information to relate the gaze angle to the distance from the cornea and retina to the electrode. Now that we have this relationship, we can progress on to the next stage of the electrode physics.

4.3.2 Electrode Physics

This next section looks into the EOG in physical detail by investigating how the signal is generated. So far we have the mechanical model of the eye and how the cornea and retina move as the gaze angle changes. Now we must combine this information with the system physics to complete the model.

The silver/silver chloride electrode is *redox* electrode. It operates by producing a voltage that is directly proportional to the electric field strength at the point of contact. Redox refers to the nature of its operation and works in the following way:

The centre of the electrode is made from silver; it has an outer coating of silver chloride. The silver chloride is exposed to the environment which contains the electric field and the silver is connected to an insulated wire that leads to the measuring equipment. The silver chloride is placed in a solution to form an electrolyte. When a salt such as silver chloride is placed in solution, chemical dissociation occurs due to the salt's weak ionic bond; this separates the metal and the non-metal and leaves the Ag^{+} and Cl^{-} ions in solution. The electrolyte's purpose is to provide a medium that has free ions which can act as electrical conductors. The chemical process is shown in equation 4.8:

$$Ag^{1+} + 1e^{-} = Ag^{0} \tag{4.8}$$

The purpose of the silver/silver chloride pairing is to provide free electrons on which work can be done by the electric field. The amount of work done on the electrode or unit charge determines the *potential (V)* of that point. The determining factor of the work done is the electric field strength as is shown in equation 4.9.

$$V = -\int \vec{E} \bullet ds \tag{4.9}$$

Thus it shows that the higher the field strength, the higher the work done in moving an electric charge and the higher the voltage that is produced by the electrode.

4.3.3 The Electric Field

The electric field generated by the corneoretinal potential is shown in figure 4.4. Also included is the distance from a local electrode to the poles of the dipole $\mathbf{d_1}$ and $\mathbf{d_2}$. The darker, inner part of the electrode is made from silver and is only electrically connected to the measurement electronics and the outer, lighter part of the electrode is made from silver chloride and is electrically connected to the skin potentials.

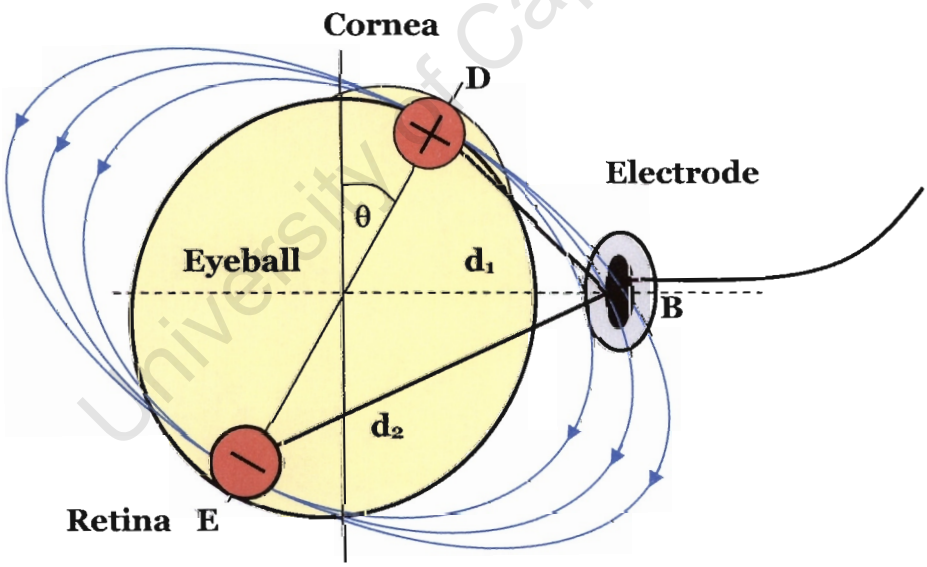

Figure 4.4: The diagram of the eye shows the ocular dipole during a clockwise gaze θ, the associated electric field, the electrode position and the distances to the poles $\mathbf{d_1}$ and $\mathbf{d_2}$.

The electric field at the electrode (point B) is dependent on two points; these two points are the positions of the positive and negative poles of the ocular dipole at

D and **E** respectively. The electric field caused by a point charge can be expressed as follows:

$$\vec{E} = \frac{q}{4\pi\varepsilon_0 r^2} \tag{4.10}$$

This means that the charges at D and E can be represented as:

$$\vec{E}_+ = \frac{q}{4\pi\varepsilon_0 (d_1)^2} \tag{4.11}$$

$$\vec{E}_- = \frac{q}{4\pi\varepsilon_0 (d_2)^2} \tag{4.12}$$

The field potential is defined as the work done on a unit charge and is expressed as:

$$V = -\int \vec{E} \bullet ds \tag{4.13}$$

Performing the integration results in the following expression for the potential V at point B,

$$V = -\int E \bullet ds = \frac{q}{4\pi\varepsilon_0}\left(\frac{d_2 - d_1}{d_2 d_1}\right) \tag{4.14}$$

We have calculated the distances $\mathbf{d_1}$ and $\mathbf{d_2}$, so the next step is to model the relationship between the output potential and gaze angle.

4.3.4 The Complete EOG Model

Up to now, we have derived all of the equations needed to create a complete mathematical model of the EOG system as drawn in figure 4.4. This model incorporates the eyeball and electrode geometric data, the electrode physics and the electric potential equations to create the complete model.

The mathematical formulae created thus far, needed to be combined to form one solitary equation that related potential and gaze angle. As the mathematical model includes complicated functions, it is difficult to analyse the function qualitatively.

It seemed that quantitative analysis would be more suited for this application and the easiest method of modelling these functions was to perform a simulation in Matlab. Looking back at figure 4.3, we chose **r** = 24.5mm and **l** = 10mm.

The angle α is shows an initial increase with increasing θ until 45° where it begins to tend to zero at 90°. The angle β is shown to steadily decrease to zero almost linearly as theta moves from 0 to 90°.

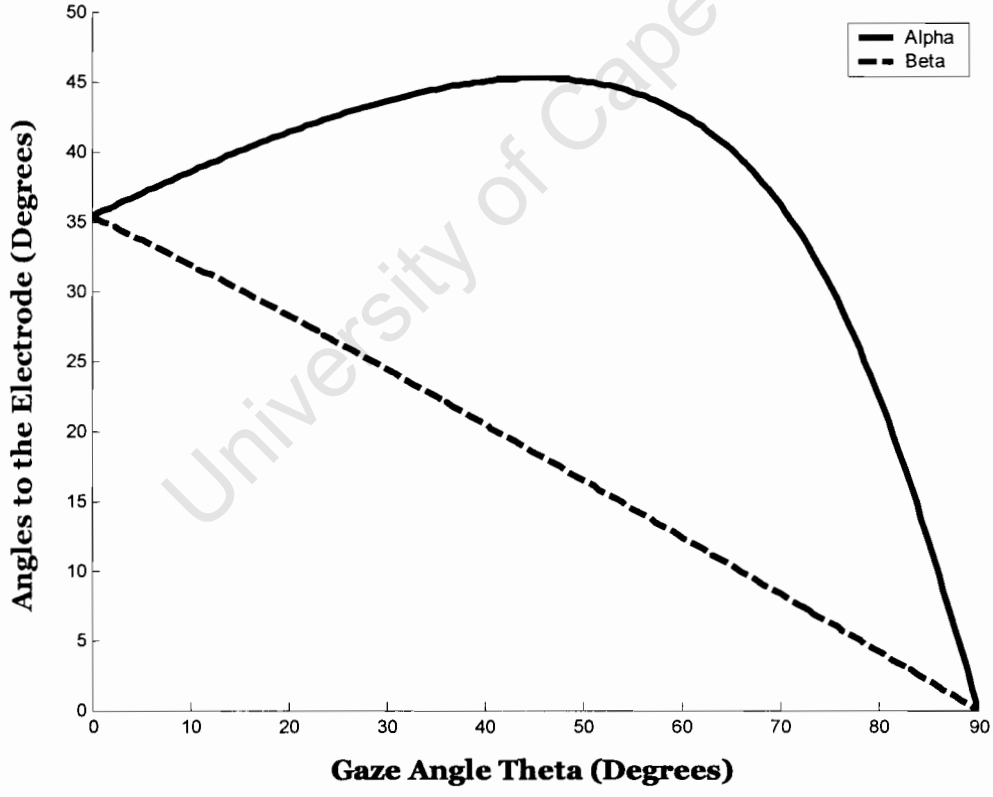

Figure 4.5: This diagram shows how the relative angles from the poles of the ocular dipole **(**β and α**)** to the electrode change with the gaze angle of the eye.

Figure 4.6 shows the distances $\mathbf{d_1}$ and $\mathbf{d_2}$, as functions of the gaze angle θ. As expected $\mathbf{d_1}$ shows a decrease with the gaze angle as it gets closer to the electrode and $\mathbf{d_2}$ displays an increase as is gets further away from the electrode as the gaze angle θ increases.

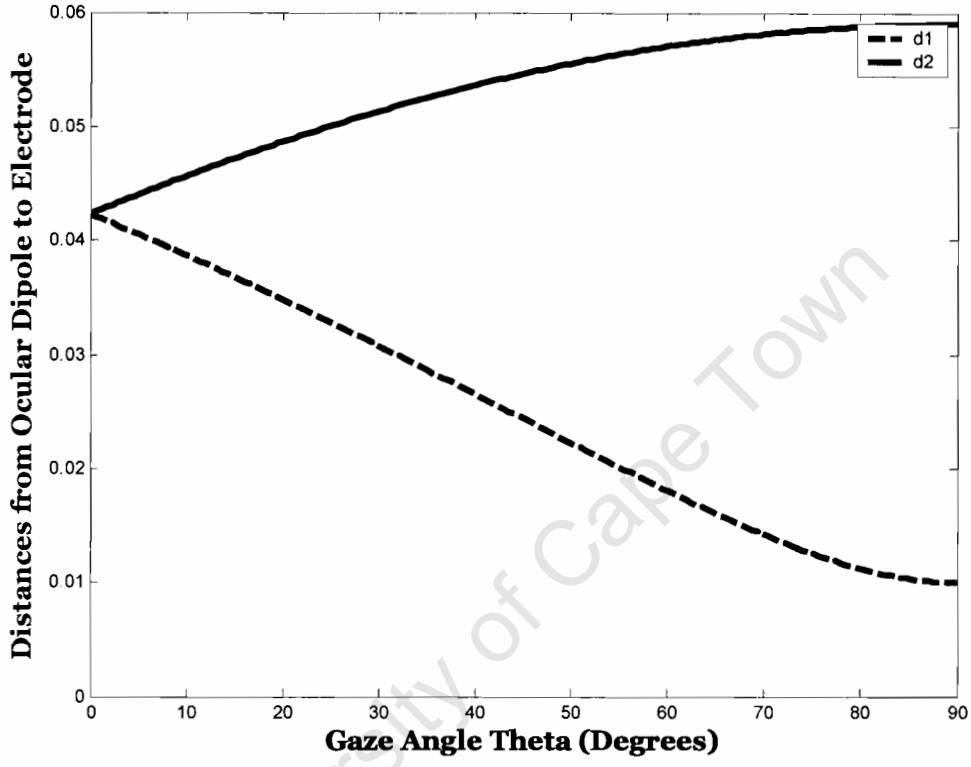

Figure 4.6: This diagram displays the dimensional relationship of the distance between the poles of the ocular dipole ($\mathbf{d_1}$ and $\mathbf{d_2}$) and the electrode.

It is clear from figure 4.5 and figure 4.6 that the relationships between the gaze angles and some of its related variables are not linear, and so we do not expect to see a linear relationship in our overall model. Figure 4.7 shows the overall relationship between the gaze angle and the potential generated by the electrode. This relationship is outlined in equation 4.14.

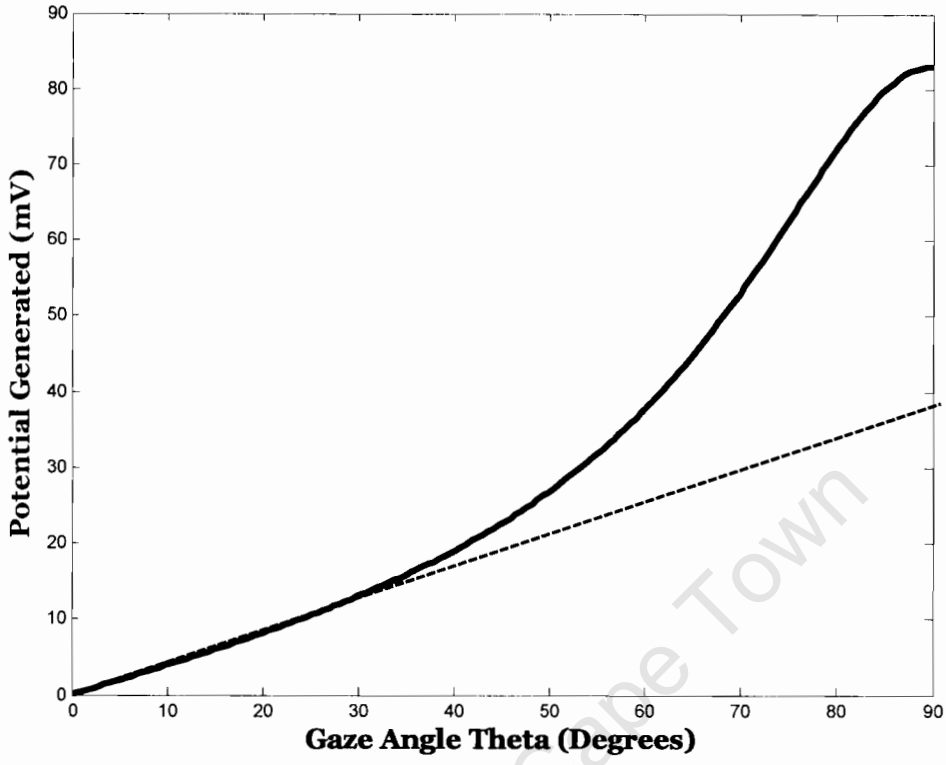

Figure 4.7: The complete EOG model relating the angle of gaze to the potential generated by the electrode.

In figure 4.7, as expected we can see an increase in the potential generated by the electrode as the gaze angle increases causing the positive cornea to move closer to the electrode and the negative retina moves away. We can see that the relationship between gaze angle and EOG potential is not linear especially in the case for $\theta > 30°$.

This non-linearity for the case of $\theta > 30°$ is documented in [2], so it is clear that this can be explained in the mechanics and physics of the EOG. Due to the fact that this is an inherent property of the EOG, the easiest method of correcting it would be to linearize the readings by passing them through the inverse function of the graph in figure 4.7. However, in this application, we are testing EOG responses that do not exceed ±10°; this places the readings in the linear zone which makes linearization unnecessary.

5 EOG Circuit Design and Construction

The decision to use a printed circuit board design was taken early in the project's development as it was the only realistic choice given the components that were being used and the desired size of the circuit board. It was by far the most space efficient method of building the EOG circuit which had to fit onto the strap of the a pair of goggles.

Printed circuit design is also more professional and robust. Tracks are used instead of wires and smaller surface mount components can be used in place of larger through-hole packages which results in reductions in thickness, width and length.

5.1 Design Objectives

The EOG circuit board was to mount onto the strap of the EOG goggles. This would enable it to receive the EOG signal from the electrodes mounted in the frame of the goggles and pass it through the instrumentation amplifier with minimal loss of the signal through wiring resistance. The signal would then be filtered, digitised and transmitted wirelessly. A diagram of this process can be seen below.

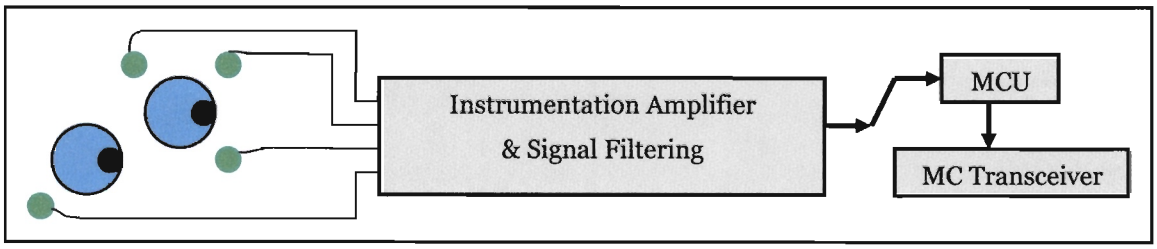

Figure 5.1: Block diagram showing a breakdown of the functions that were needed to perform in the EOG board.

The size constraints were to ensure that the board mounted comfortably onto the goggles with minimal interference to the subject.

5.2 Block Circuit Designs

Each specific component of the circuit board has individual design needs. There are three main blocks which include the analog amplification and filtering of the EOG, the digital requirements of the MCU and the wireless MC13192. The following sections outline the design of each block labelled in figure 5.1, and list their specific circuit requirements.

5.2.1 Electro-Oculogram Circuit

The EOG signal is transmitted through a six pin connector mounted onto the board via a six strand parallel signal wire. This wire is protected against electromagnetic interference with metal shielding. Two of these signals are grounded to the battery terminal in order to act as earthing electrodes. The other four signals are connected to the input pins of two AD620 Instrumentation Amplifiers.

The AD620 instrumentation amplifiers are differential amplifiers with two pins that specify the gain depending on the resistance placed between them. In this case, a 1kΩ potentiometer was used so that the gain could be varied.

The next stage is to low pass filter the signal to eliminate any other interference signals. The cut off frequency was selected to be 80Hz, as this is half the sampling frequency. At this point, it was decided to pass the signals through another operational amplifier that could add a potentiometer adjusted variable DC signal to the EOG signal. The gain of this operational amplifier could also be

adjusted to fit the signal within the A/D converter limits. The surface mount quad package used was an OP490. This marks the end of the analog phase.

5.2.2 MC9S08 Microprocessor

The microprocessor used in the EOG signal generation circuit board is a Freescale MC9S08GT16. It is required to digitise two channels of EOG information, convert them into a packet by appending an 'x' and 'y' symbol before each one and then interacting with the Freescale MC13192 transceiver to transmit the signals. The circuit requirements include:

- Power supply connection to the power pins and the voltage limit pins of the A/D converter.
- External clock pin which is connected to the output clock pin of the MC13192. This ensures accurate timing between the two components.
- Reset pin connected to an external pushbutton switch.
- Connection to a six pin connector that connects the supply, ground, reset and programming pins to the BDM multilink programmer.
- Four wire SPI connection (SS, MOSI, MISO, CLK) to the MC13192.
- A/D connection to the output pins of the OP490 to receive the EOG signal.

Figure 5.2 overleaf shows all of the aforementioned connections in a circuit diagram. This is the recommended connection diagram from Freescale [34].

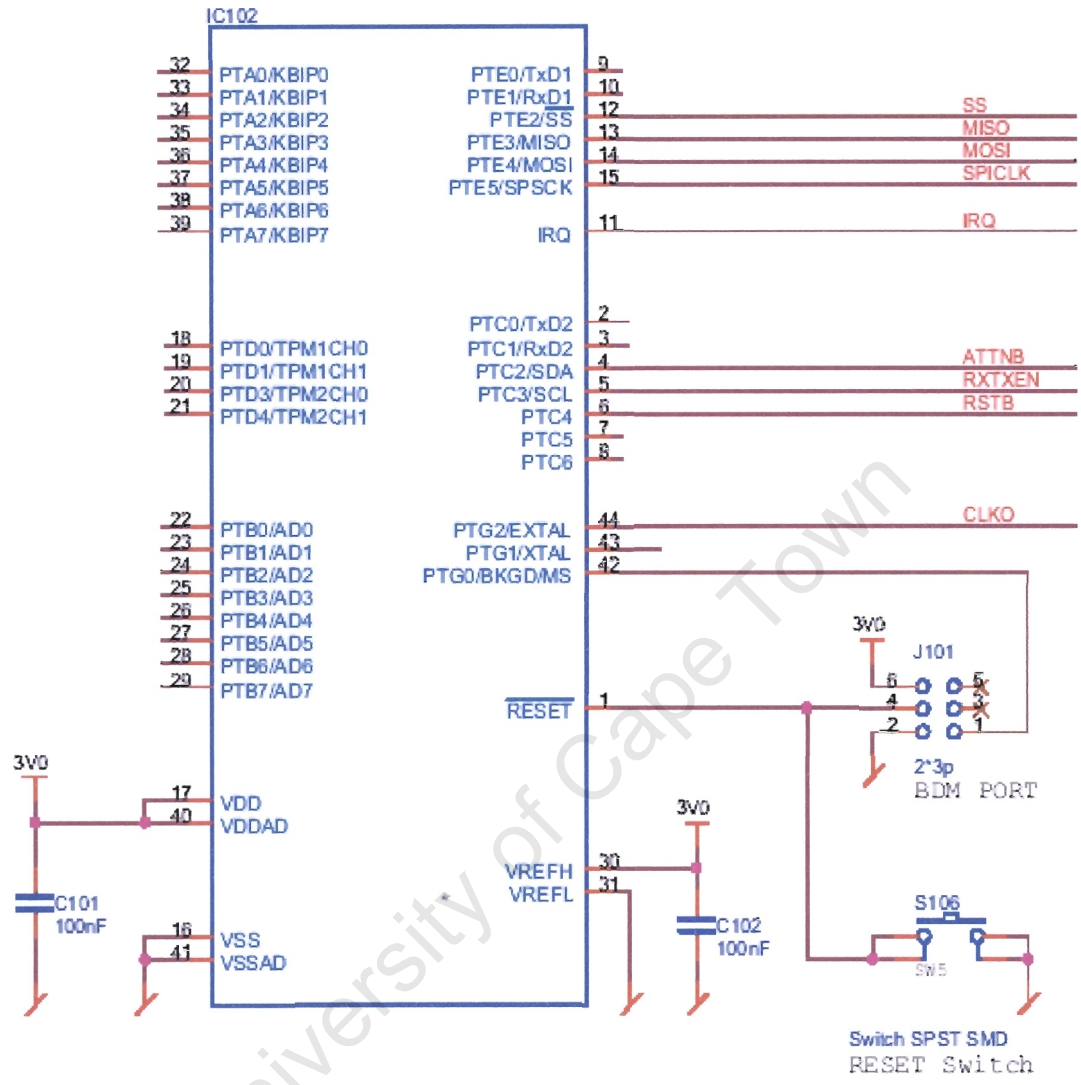

Figure 5.2: A diagram showing MCS908GT16 and the fundamental connections to be made for normal operation [34].

5.2.3 Freescale MC13192 Transceiver

The Freescale MC13192 transceiver chip is a small (5x5mm) surface mount package. As a result of its size, the MC13192 had to be machine soldered and the surrounding track widths were the smallest allowable by the printed circuit board manufacturer.

The circuit requirements include:

- Supply and Ground connections
- Four wire SPI connection (SS, MOSI, MISO, CLK) to the MC13192
- External Input Clock signal
- Antenna transmit and receive connection
- Microstrip connections

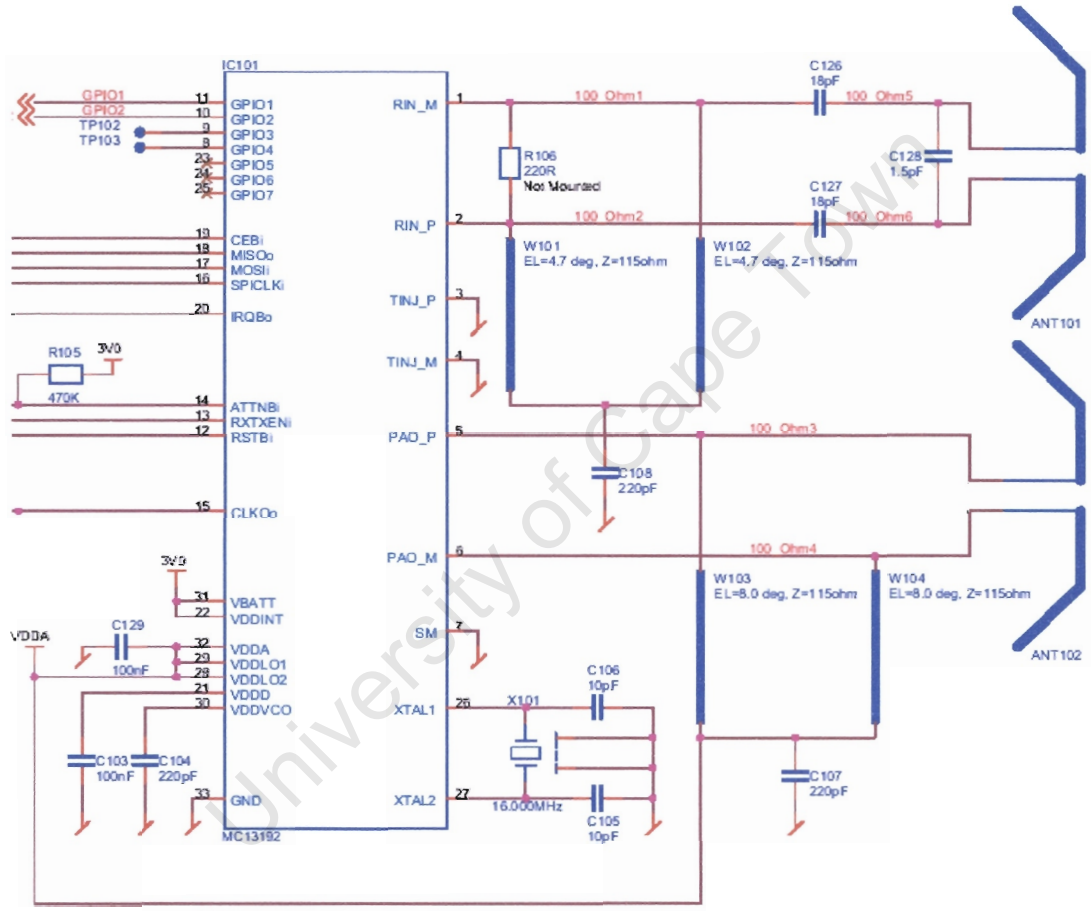

Figure 5.3: A diagram showing MC13192 and the connections to be made for normal operation [34].

5.2.3.1 Microstrip Impedance

At 2.4 GHz, the transceiver chip experiences some input/output impedance when transmitting and receiving signals. The source of this impedance is within the

chip itself and despite being minimal; the extremity of the frequency renders it significant to the output power. The microstrip is designed to have an impedance equal to the negative of the imaginary part of the output impedance of the MC13192 to in order to maximize the output power.

When designing a Printed Circuit Board, there is a software tool used for calculating the microstrip impedance that takes board thickness, electrical length, phase angle and track width into account. The program produces the length and width of the track to be used in order to achieve the desired impedance.

Due to the minimal range requirements, the antenna that was used was printed onto the board itself. It was a very convenient place for the antenna as it required little extra space.

5.2.3.2 External Crystal Oscillator

The external crystal oscillator used as the clock input for the MCU and MC13192 that was used was a CFPS-73, made by Cmac. It is a four pin, 3.3V surface mount package which met the accuracy requirements of the MC13192. It has a Frequency Stability of 25 ppm and operating range of 0-70°.

5.2.4 General Design Notes

Due to the variety of signals present in a board such as the EOG board, it is important to consider the effects of coupling. If a high speed digital signal is being transmitted along a track that lies close to a slow-moving analog signal, there can be some crosstalk which will compromise both signals. It is important therefore, to isolate the digital and analog signals and to use a decoupling capacitor to ground all signals that need to be stable such as the supply rails.

6 MICROPROCESSOR USE AND PROGRAMMING

The EOG system required microprocessor technology in order to complete tasks in digitisation, wireless transmission and reception, serial and parallel communications. Essentially, the microprocessor was needed to be at the heart of each data transfer process.

The purpose of this chapter is to discuss what the EOG system design required of the microprocessor, how we chose which microprocessor to use and how we made use of the microprocessor in various applications.

6.1 Processor Requirements of the Wireless EOG

The wireless EOG system design was based on an analog data input path. The first step in the EOG chain was to acquire a biological signal and filter it. Once this signal conditioning had been performed, it was necessary to convert it into a digital signal for the rest of the signal transfer process which is entirely controlled by two microprocessors.

Overleaf, figure 6.1 shows all of the data transfer processes in the complete design showing the two microprocessors, and the functions that they are required to perform.

The EOG signal is digitised and converted into a packet which is sent over SPI to the transceiver to be wirelessly transmitted. It received by a similar transceiver and then transmitted over SPI to the second microprocessor which combines the information with the visual test stimulus data to create the complete EOG packet to be sent to the PC using the SCI module.

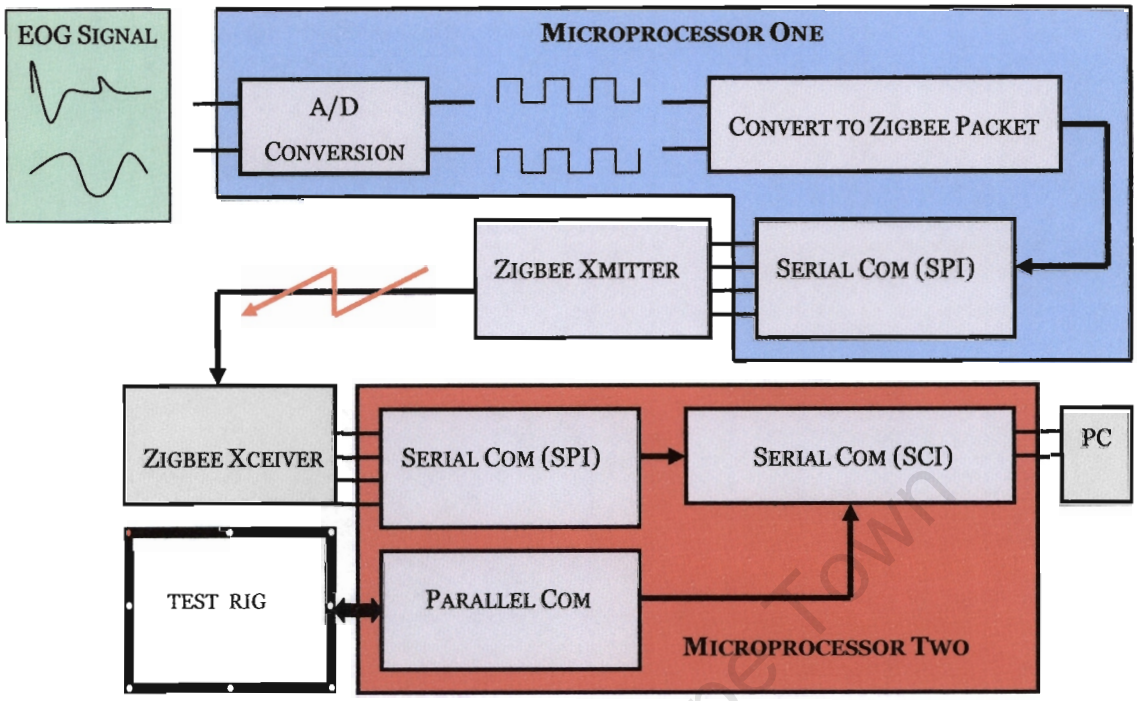

Figure 6.1: The EOG System as regards Data Transfer, showing the roles that the two microprocessors play highlighted in blue and red.

In order to the complete the process, the following process requirements of the microprocessor were to include the following features:

- 2 Channels of 10-bit analog to digital conversion
- A serial communication module (SCI)
- A serial peripheral interface module (SPI)
- An external input clock pin
- High resolution timing functions
- 20 General purpose input output pins
- Surface mount availablility
- At least 16K Flash onboard to load the Zigbee Stack and have enough space for a program
- Be able to be programmed in C
- Low Power

These are not stringent microprocessor requirements and there are many different microprocessors that suit this application. The next section will outline the reasons for the choice of microprocessor.

6.2 Microprocessor Design Choice

The choice of microprocessor and the choice of wireless module were interlinked. At the time of making a decision, a development board made to demonstrate the Freescale MC13192 2.4 GHz Transceiver was available. The documentation that accompanied the board included datasheets of the components used, circuit diagram schematics, sample programs and sample code. As this development information was available on the Freescale platform, it was decided to use the MC9S08GTXX series microcontroller.

This microcontroller contains all the features of the HCS08, but includes extra features that suited my application in particular such as:

- On chip programmable flash memory
- On chip RAM
- 8-channel 10-bit A/D converter (ATD)
- 2 Serial communications interface modules (SCI)
- Serial peripheral interface module (SPI)
- External input clock pin
- 16 Bit timer modules
- 36 General purpose input/output pins
- 44-Pin quad flat surface mount package

The exact device that was used for the EOG data capturing board which transmitted the EOG signal was the MC9S08GT16. This particular chip has 16k Flash, 1K RAM, 36 I/O Pins and two 2-channel 16 bit timers. The device used on the development board which was used to receive the wireless signal was a

MC9S08GT60, which has a memory upgrade on the GT16 with 60kB Flash and 4kB RAM while the other features remain the same.

6.3 Hardware Specifications of the MC9S08GT16

The MC9S08GT16 microprocessor was easy to integrate into the circuit design as a circuit diagram indicating pins and connections is available in the data sheet [32]. In this application, these connections included:

- Two power and two ground connection.
- The A/D converter high and low limits
- External input clock pin
- Programming pins
- Reset switch
- Four wire connection of SPI to MC13192
- GPIO pins

The package used was a surface mount package. This added to the compactness of the circuit board while remaining robust. It is however, more difficult to solder and remove if necessary.

6.4 Programming of the Microprocessor

Programming the MC9S08GTXX was performed using Metrowerks Code Warrior and the programs were written in assembler and C. Mounted on the circuit board was a 6-pin connector block into which the BDM Multilink programmer was plugged. This was used to download programs from Code Warrior via the BDM Multilink.

The BDM Multilink programmer works with a USB PC interface which connects to code warrior. The code is is translated into serial information and transferred through the USB port to the programmer where it is then downloaded onto the microprocessor through the programming port. This 6 pin connector connects to 4 pins. These pins are the reset, ground, supply and programming pins. Two of the pins are left unconnected.

7 ZIGBEE WIRELESS DATA TRANSFER AND SMAC

An integral part of the project was to allow the subject freedom of movement without any measurement wires leading from the EOG apparatus to an instrumentation station. This was an important specification as sporting applications need versatility. It was for this reason that it was decided that the EOG data would be transmitted over a wireless link to a receiver station.

7.1 Wireless Requirements of the EOG System

The EOG system required a wireless transmitter that was small, low power and easy to use. It needed to be able to operate with a printed antenna, as using minimal space was a priority. It was necessary to be able to transmit data at 6.44 kbps over a distance of less than 10m in order to be able to keep up with the sampling frequency of the EOG data. Essentially, the data throughput demands were small, whereas space and ease of use were of greater importance.

7.2 Freescale MC13192 Transceiver

The product that was chosen was the Freescale MC13192 transceiver. It was an easily available technology at the time of development and possessed all of the capability to comfortably satisfy the wireless data transfer requirements of the project.

7.2.1 Introduction to the MC13192

The Freescale MC13192 is a low power, short range, 2.4 GHz transceiver which contains a complete 802.15.4 physical layer modem designed for the

IEEE 802.15.4 wireless standard supporting star and mesh networks [32]. It is designed to be combined with a microcontroller in order to provide a complete solution for short-range wireless data links. The communication between the MCU and the MC13192 is achieved with a four pin SPI connection interface. This enables the designer the right to a maximum choice of processors. Depending on the software that the developer would like to use, the MC13192 can be configured to handle anything from simple point to point contact to Zigbee Networking.

Freescale advertises that this transceiver could be used in the following applications:

- Remote control and wire replacement in industrial systems such as wireless sensor systems
- Factory automation and control
- Heating and cooling
- Inventory management and RFID tagging

The transceiver includes a low noise amplifier, 1.0mW PA, VCO and full spread spectrum encoding and decoding. The device supports 250 kbps O-OPSK data in 5.0 MHz channels as per the IEEE 802.15.4 standard. SPI is used for Rx and Tx data transfer and control [32].

7.2.2 Using the MC13192 with EOG

The wireless EOG system design needed this transceiver to perform in its most basic mode. It needed to transfer between two nodes no more than 10m apart at a rate of 6.44 kbps. By wireless standards, this is a low data rate and a very short transmission distance. Therefore, the MC13192 was more than capable of satisfying these needs.

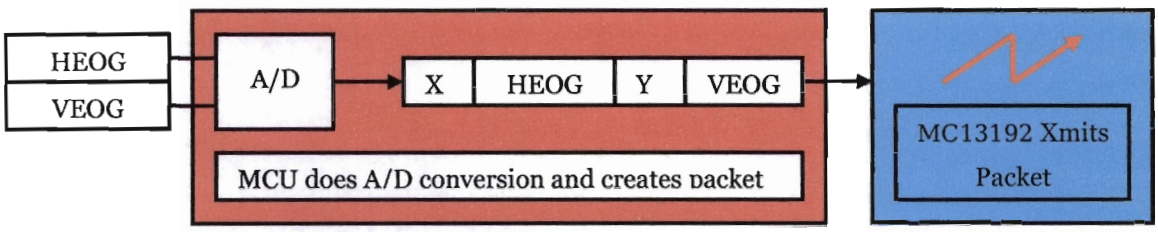

Figure 7.1: The wireless EOG data transfer process.

In figure 7.1, the data transmission process begins with the EOG data being captured in two channels (HEOG, VEOG), it is then digitised with the A/D converter. The digital data is then packeted by appending a prefix to label each byte before being transferred between the MCU and the MC13192 over an SPI connection, where the data is transmitted to the listening node.

7.3 Programming with SMAC

In wireless applications, the Freescale MCU and MC13192 components act in unison. The MCU is the configurable, programmable component while the MC13192 receives and transmits. These two components are a powerful combination and can be used to suit a large variety of applications. It is for this reason that Freescale released SMAC.

SMAC (Simple Media Access Controller) is a C based code stack to be used as sample source code for developers of RF transceiver technology. This code can be modified to be used on any RF transceiver developmental hardware provided that the MC13192 and an HCS08 MCU was used.

The SMAC contains a stack which is loaded onto the microprocessor core which enables it to communicate with the RF transceiver. Other features include:

- Small footprint – 2K flash, 10 bytes RAM
- Low power bi-directional link

- Portable C source code can be used on a variety of core processors
- Automatic Frame Check Sequence for error detection
- Up to 123 bytes of payload data

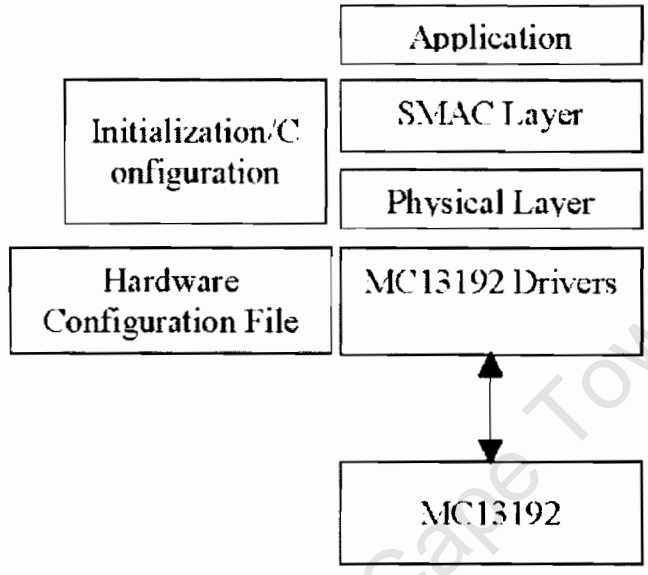

Figure 7.2: Taken from [31], this is the Block Diagram of the SMAC showing how its structure.

The SMAC software provides the wireless gateway from the application level through to the hardware level. In the main C program a single line of code can perform a wireless command which is then passed on to the lower levels to finally perform the transmission at the hardware level by communicating with the MC13192 via the SPI.

7.3.1 Amendments to the SMAC

The sample code was helpful in getting started and it compiled and ran on the development kits which were used as receivers. It was more complicated when transferred to the EOG board, as there are a few differences in the hardware. In this application, the important modifications to the SMAC code were to include the following changes:

- SMAC is initially set up to operate an MC9S08GT60, where my application used a MC9S08GT16. This modification involved changing the flash and RAM address limits.
- The GPIO ports for use in communication with the transceiver had to be modified to incorporate my design. The port names are hard coded in the SMAC, and these had to be changed.

When these problems were cleared up, the two platforms communicated without difficulty.

8 THE VISUAL TEST FACILITY

The implementation of the visual test facility is the last stage to be completed and acts as the yardstick on which to measure whether the EOG technology is a feasible option by which to measure vision in high performance sport. There are various types of testing that can be carried out, the details of which are discussed in this chapter.

8.1 Types of Eye Movement Tests

There are two different types of testing that were initially intended to be carried out. The first tests a pursuit-type of movement and the second tests a saccadic type of movement. The next two sections will discuss each one.

8.1.1 Pursuit Eye Movement Test

The pursuit eye movement test (PEMT) is concerned with ascertaining how good a subject is at tracking a moving target with their eyes. An example is if a bird is flying overhead and you are watching it, how good your eyes are at performing the smooth pursuit eye movement that is necessary to remain focused on the bird at all times is what the PEMT assesses.

In order for your eyes to have a 100% test record in a PEMT, it has to be shown that the direction of your gaze was always within 3° of the stimulus [29]. If your gaze falls out of this range for any length of time, the test score drops.

Given that electro-oculography has an accuracy of 2° at best after eradicating the DC slow potential drift, it makes for a very difficult test to perform using EOG.

The PEMT is also not designed to test fast pursuit movements, so it is not all that relevant in the field of sports vision.

It has been shown that in cricket [31], when a delivery is bowled, a batsman only takes two samples of the trajectory of the delivery. The first sample is as the bowler releases the ball and the second sample occurs just before the delivery bounces. This shows that when the pursuit speeds are as high as that, the eye uses saccadic eye movements to track a moving target.

It was on the basis of this logic that it was decided to focus on saccadic eye performance testing as it more suitably matched the application and the hardware.

8.1.2 Saccadic Eye Movement Test

The electro-oculogram is the most primary form of eye movement detection. Unlike infrared detection, there is very little processing that occurs between when the eye moves and the signal is measured. It is for this reason that the transient analysis of the EOG is especially accurate, as there is little or no intermediate transfer functions to affect the result.

In the Saccadic Eye Movement Test (SEMT), the most important information is the dynamic, transient response of the eye. This means that we are looking for the derivative with respect to time, and not the DC position (as in PEMT). This suits the EOG signal because we would like to eradicate the DC as much as possible as this is the portion of the signal that varies unpredictably.

The SEMT is concerned the individual performance of one *saccade*. One theory of improving a high performance sportsperson says that by increasing the performance of a saccade and by increasing the frequency at which somebody is

able to perform a string of saccades, your overall vision is improving because you have a higher visual "refresh rate" [31].

An example of where this might be applicable is in a rugby game. A player is in close quarters, possibly in a ruck or maul where he is focused on his immediate surroundings and unable to see much beyond that. In the next moment, he has broken free and is in a completely new visual surrounding with space as he crosses the opponent's gain line. In this moment he has to register all of the brand new visual information that surrounds him in order to make the best decision as to his next move. He might have a wing on his left; tacklers approaching from left, right and other players in support. The faster that he can make the necessary saccadic eye movements, the faster he will have all the peripheral information at hand and the more informed he will be when making decisions. So it would seem that saccadic eye performance plays a very important role in some sports.

The SEMT is concerned with getting the subject to rapidly move their eyes from one target (light source) to another. In this project, the light sources were LEDs set in a frame. The subject would then focus on that light source until another one illuminates. The eye movement data during this test is logged along with the light source data and timing information.

The things to look out for in the SEMT are the eye movement dynamics such as how fast the eyes move (maximum eye velocity), the time taken for the subject to react to the visual stimulus (saccadic latency), overshoot and oscillation.

8.2 Objectives of the Visual Test Facility

The objectives of the visual test facility are essentially to set up a SEMT that has a few variables that can be easily changed. This gives the tester a few different

options in order to isolate areas of vision that he is trying to test. These variables are:

- Time length of the saccade
- Light source positions
- Randomness of the timing and firing of the light sources
- Pre programmed light firing sequences

The test facility must contain functionality that allows for testing in the X and Y plane so that horizontal and vertical movement can be independently assessed. It is also important to use electronics that has a small time delay from the time of switching to the firing time.

8.3 Design

Figure 8.1 shows a simple square frame. The frame is painted black to increase the contrast of the firing red LED. Embedded into this frame are a series of 8 LEDs which are placed on the four corners of the frame as well as at the midpoints of each frame side. The frame size was designed in such a way that the subject's gaze never exceeds 30°.

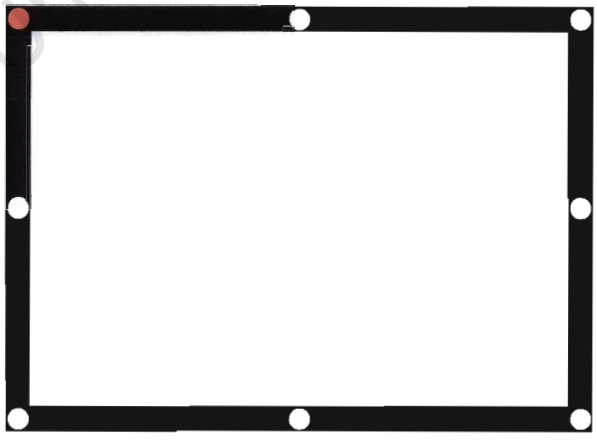

Figure 8.1: A diagram depicting the test facility LED frame with the top left LED firing.

The 8 LEDs are then connected over a parallel transmission link to a series of transistor driver circuits which are controlled by the output pins on the test facility controller. This allows for total control of the Test facility by the microcontroller.

The various programs that were loaded into the Microprocessor were activated by pressing one of four push button switches. These push button switches would activate certain pre-programmed routines. The routines are listed as follows

8.3.1 Calibration

The calibration routine was run with the LEDs following a clockwise path for the subject to track. This was an easy routine to follow as the subject knew where the lights were going to fire next and at what timing interval. It was designed to be easy to follow so that online calibration of the circuitry could be performed without tiring the subject. The calibration ensured that the full range of the A/D converter could be utilized.

Included within the calibration routine is assessment of the level of crosstalk that exists between the two EOG channels. This phenomenon is explained in section 4.3.2 which discusses electrode placement. Due to the calibration firing sequence chosen, we should detect movement in one channel at a time. This allows us to measure whether there is a signal in more than one channel, in which case we can make the necessary allowances for crosstalk.

8.3.2 Opposite Corners

The opposite corners routine was setup as quite a challenging routine that would show whether there was a discrepancy between a subject's horizontal and vertical eye movement ability. It was expected that horizontal eye movement would be

more developed due to the training of reading. As the subject's gaze would traverse the frame corners, both channels would be expected to show a movement.

8.3.3 Consecutive Midpoints

The midpoint test is generated as a pure SEMT that tests horizontal and vertical eye movement separately. In this test, the horizontal LEDs are fired twice each alternately followed by the vertical LEDs completing the same sequence. The timing and firing sequence is consistent and does not change.

8.3.4 Random Firing at Random Intervals

This test is the most commonly used SEMT as it gives no pattern in time or position. In this test the lights fire at random intervals and random positions which simulates the most realistic SEMT. In this test, eye movement as well as reaction time is assessed.

8.4 Visual Test Facility Controller Operation

The test facility is the central control point of the whole EOG data logging system. It facilitates the type of test that is being used and runs the test while logging the EOG data and transmitting it to the serial communications port. In figure 8.2, the sequence of programming events is outlined.

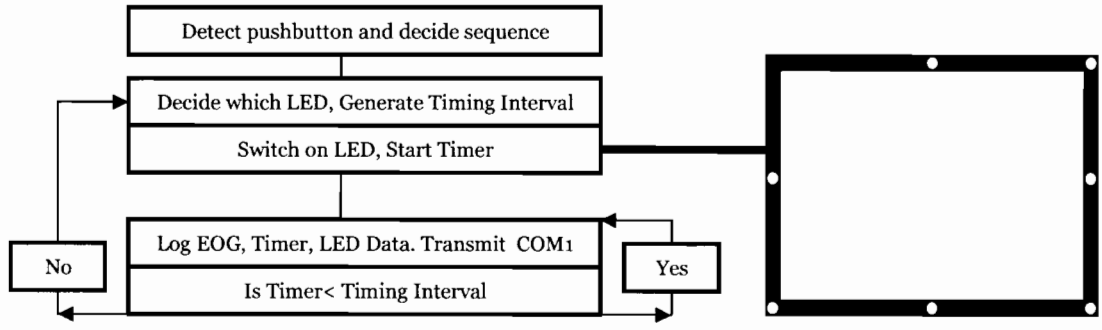

Figure 8.2: The programming map of the events that facilitate the Test facility operation and data communications.

Figure 8.2 outlines the steps of the program that controls the test facility controller and EOG data logger. The program is compiled from C and programmed using Metrowerks.

The user has the choice of which test to select by pressing one of four pushbuttons. When a sequence is selected, the program begins a cycle of firing an LED for a predetermined time while the subject (who is wearing the goggles) is required to visually track the LED sequence as fast and accurately as possible. The EOG data is logged and transmitted with the LED and timing data to the PC.

9 HIGH LEVEL SOFTWARE

When all of the hardware has been implemented, and it works to ensure that the integrity of the data remains intact throughout the capturing and transceiving process, the end result is a large text file. This text file contains the raw data collected 140 times a second of horizontal and vertical eye movement, visual stimuli, and elapsed time. These pieces of information comprise the total dataset that this project undertook to capture.

When the data is in this format, then we can use high level programming to perform a host of data analysis operations. These operations help us to extract the information that we want. This chapter will discuss the methods of data analysis used in this project.

9.1 Serial Information Data Capture

The wireless receiver module is responsible for transmitting the data that it gathers from the EOG unit. The receiver module is shown in figure 9.1 in green, depicting the data transmission pathways.

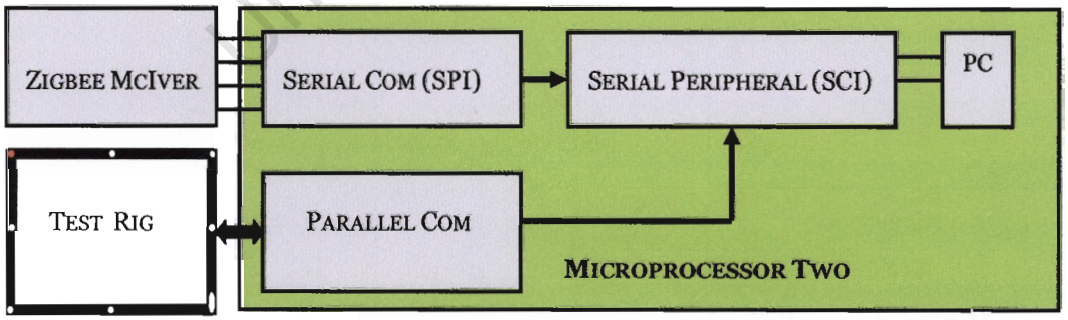

Figure 9.1: The wireless receiver module accepts data from the EOG interface and transmits the data to the PC via a serial uplink.

The complete packet contains EOG signal information, timing and visual stimuli information, which is transmitted to the test facility unit and the PC. This packet contains five 8-bit fields which are organised as shown in the table below.

Type of Data	Data Size
Horizontal EOG	8 bit
Vertical EOG	8 bit
Which LED Fires	8 bit
Timer Channel (H and L)	16 bit

Table 9-1: The structure of the final EOG diagnostics packet.

The data is transmitted at a baud rate of 38400 bps.

A visual basic program reads the serial data. Visual Basic was used as it is an easy and convenient high level program with sample code available.

Visual Basic has a control called "serial comms". It is box that placed onto the GUI which can be configured according to the data you expect to receive. These configurations include the data size, packet length, baud rate, stop bits etc. In order to use the serial communications port, it first has to be opened. When the data is received by Visual Basic, the 8-bit information is represented in the corresponding ASCII code. A simple conversion process to change it into a number and write to text file completes the process that converts the serial data into a workable format.

9.2 Using MATLAB for Data Analysis

The raw data contained in a test file needs to be processed in order to be presented for analysis. The data has been passed through some forms of electronic signal conditioning, but further processing is necessary to produce the

final product. The slow DC potential signal drift has to be removed and some low pass filtering is necessary to clean the signal. At this stage, it is desirable to have an automated EOG analysis process that can process the data and determine certain eye parameters automatically.

9.2.1 Calibration

In order for our data to be analysed and interpreted by vision coaches, it needs to be in a form that is universally understandable. It needs to be converted from binary format into real world variables such as degrees and seconds.

9.2.1.1 EOG Calibration

In this application, each test has to be individually calibrated. This involves ascertaining the limits of the signals and back propagating these perimeter values to correlate them with the gaze angle variable.

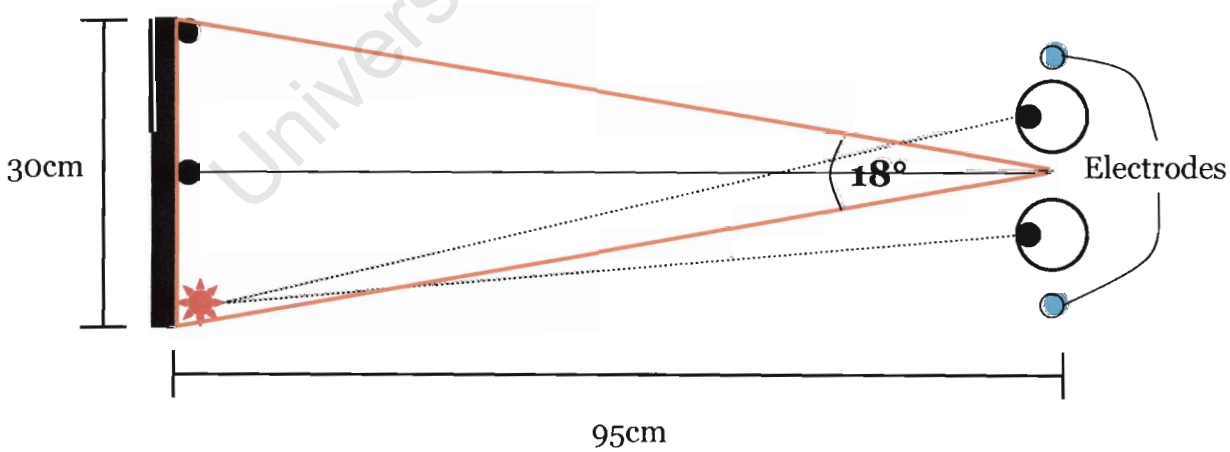

Figure 9.2: The limits of eye movement in a test environment are shown. This part of the calibration process informs the tester of the maximum eye rotation angles that he can expect from the EOG readings.

If we have a relationship between the limits of the test and the limits of the signal, then we have a value that transforms our voltage reading into an actual gaze angle. In this application, the transformation can be assumed to be linear as the gaze angles are lower than ±10°.

Figure 9.2 shows the geometric positioning of the eyes relative to the visual stimulus test facility. It is clear from the diagram that in this particular test, the maximum angle of rotation will be ±9°. The knowledge of this maximum angle allows the tester to correlate it with the LED that has been instructed to shine at that time. An example of this follows:

> *In **figure 9.2**, we will look at three instants **t=37s**, **t=40s** and **t=42s**. At each of these instants, we have the information that tells us which LED was on at that time. We also have the maximum gaze angles that the subject was expected to make during the test. Using this information, we can record that at **t=37s**, the subject was looking straight ahead, at **t=40s**, the subject was looking **9°** to the left and at **t=42s**, the subject was looking **9°** to the right.*

When Matlab receives the information, the horizontal and vertical EOG readings are expressed as a number between 0 and 256. The calibration gives us a relationship between this binary number and the angle of gaze. Studies have shown that the achievable accuracy is seldom lower than 2° [1], which is acceptable as we are mostly interested in the transient behaviour of the eye.

9.2.1.2 Time Calibration

The timing data is stored as a 16-bit number made up of two 8-bit registers. The counter reaches its maximum value approximately every second where it begins from zero again. This timing data needs to be converted into continuous timing in order to be read easily from a graph. This is achieved by a process of converting the 16 bit number into base 10 and ensuring that each time the timer restarts, a new time variable keeps counting up.

9.2.1.3 LED Data Calibration

The information pertaining to which LED is illuminated is expressed as a base two number in the same format as the EOG readings. The LED data is transmitted as a base 2 number that represents which LED is firing. In order to receive a number from 1 to 8 corresponding to the relevant LED, a simple logarithm base 2 function is performed on the original number.

9.2.2 Removing the Slow DC Potential Drift

The signal drift is a slow moving potential that is appended to the dynamic EOG signals. This underlying DC signal makes automated signal processing difficult, as the signal's behaviour is large and unpredictable. The tactic for removing this signal was based on a model similar to that used in [5]. This method involved isolating the slow moving signal and subtracting it from the original waveform.

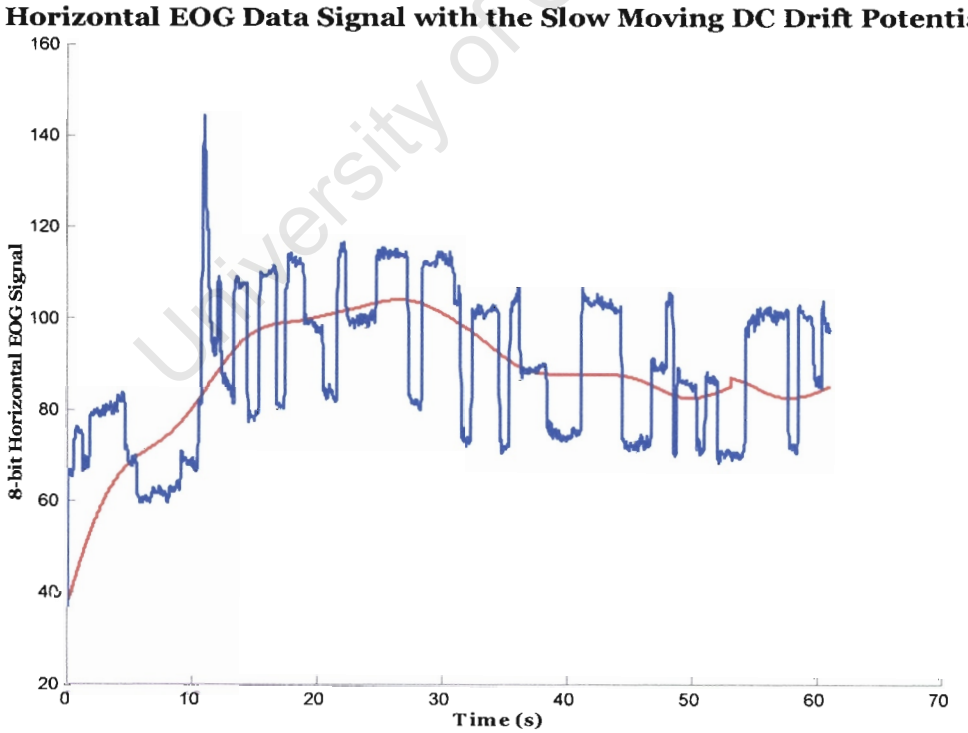

Figure 9.3: This graph, generated by MATLAB, depicts an original unconditioned HEOG signal in blue, with the slow moving DC potential shown in red.

Figure 9.3 shows Horizontal EOG data in blue as it is received by MATLAB. The blue HEOG signal is the response of a subject who was completing a Saccadic Eye Movement Test. These horizontal eye movement readings depict left, right and straight ahead eye positions.

In the graph, it can be observed that the range of the HEOG signal remains constant, however the region in which the signal moves fluctuates slowly with time. This fluctuation is due to the DC drift phenomenon. The red line is the result of a low pass filter calculation that produces the underlying DC signal. The function used to low pass filter the signal was the following:

$$w[n+1] = 0.5(1 - \cos(\frac{2\pi n}{N})) \tag{9.1}$$

The advantage of this signal is that outside of the DC slow moving signal's bandwidth the signals that we're interested in are quite far away. This enables us to use this low pass filter function as the slow decay of the frequency sidebands has no bearing on the EOG signal.

At this stage we have the original waveform and a component of the waveform that we would like to eradicate. The next step is to subtract the Slow Moving DC Drift Signal from the original signal. This process leaves us with the EOG signal without the drift shown over leaf in figure 9.4.

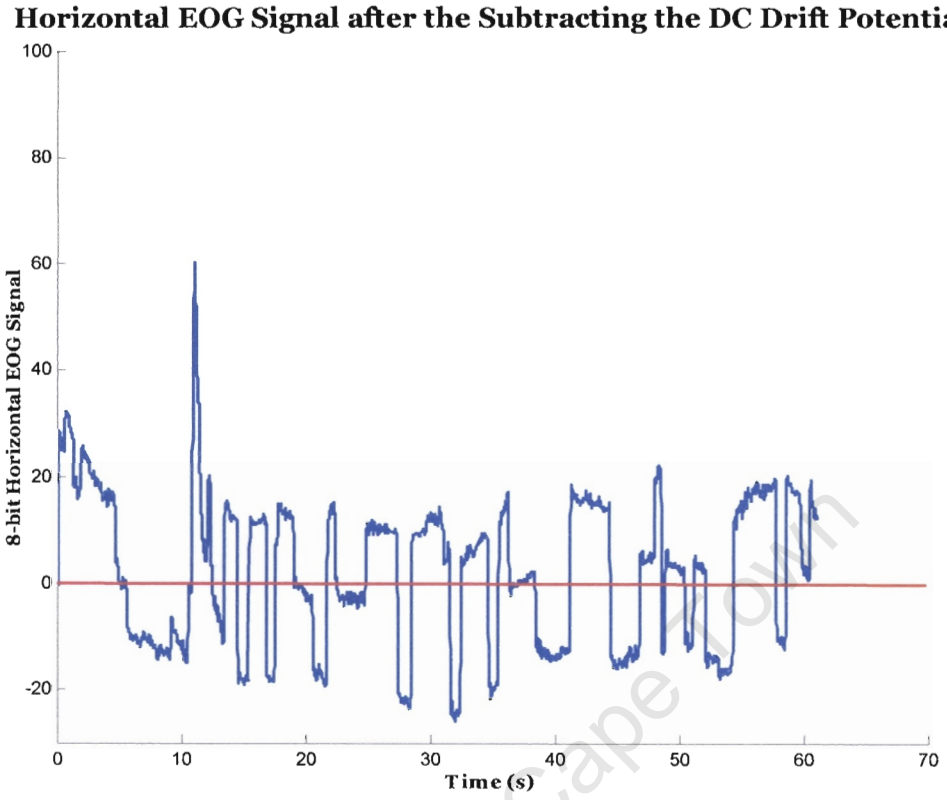

Figure 9.4: The Horizontal EOG Signal is shown with the DC Drift removed.

In order for us to be able to automate the process of evaluating the eye movement parameters, we have to be able to feed data that is consistent with a particular model. A large part of this model would include having uniform data that is centred about one fixed value without any drift. The modified signal is in a better position for us to be able to run a program that can ascertain the dynamic parameters of the eye.

10 RESULTS

The following chapter will disclose results produced by the wireless EOG device. The test environment was set up as described in the previous chapter with a random saccadic eye movement test being used (SEMT). In this test we can measure various parameters associated with the eye such as saccadic latency, maximum saccade speed, overshoot, undershoot and oscillation. The reason for using this test is due to compatibility with the results of previously published tests performed with other diagnostic equipment. This ensures that we can compare our test with others to ascertain the integrity of our eye movement data.

The purpose of the test was to evaluate the hardware for:

- Robustness and suitability of the goggles to be used in a sporting environment
- Analog eradication of the slow moving DC drift potential
- The wireless transmission capability and range
- Performance of the microcontroller
- High level software competence
- Overall transportation of a coherent EOG signal

All these factors are responsible for delivering an ideal EOG signal.

10.1 EOG Goggles

The electrode housing in this application consisted of a pair of goggles. The electrodes and their wiring were sunk into the spongy frame as can be seen in the pictures below.

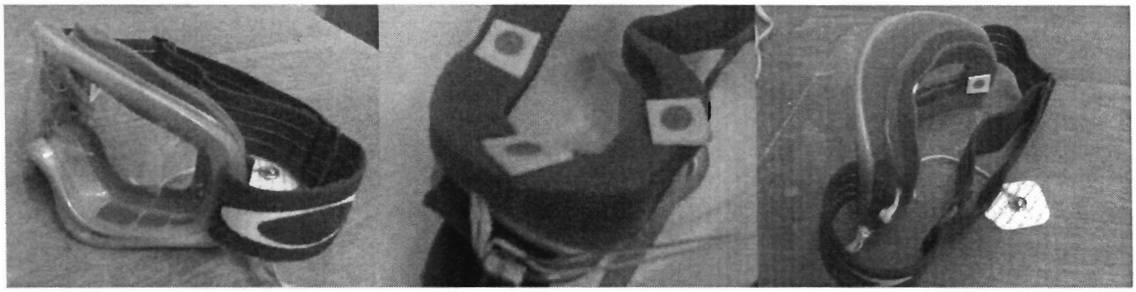

Figure 10.1: Three views of the EOG goggles showing the electrode placement in the frame.

10.1.1 Goggle Positives

The goggles were lightweight and with the wide elastic strap, they were very comfortable to wear. The sponge is soft and the plastic frame is quite flexible which enables a subject to wear them for long periods without discomfort. The wide strap is helpful as it provides a good base for the printed circuit board to be mounted on as can be seen below.

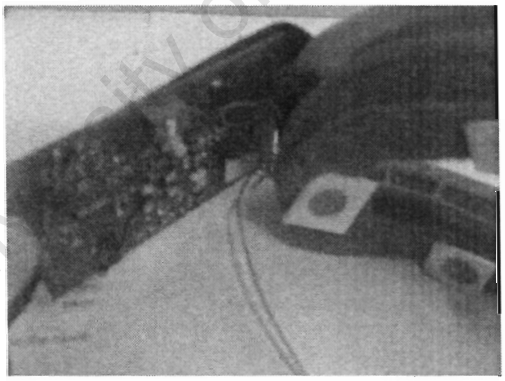

Figure 10.2: A view of the EOG PCB mounted onto the strap of the Goggles.

The wireless ability of the goggles proved to be essential as the various tests were performed. In the early stages of the project, tests were done using wired electrodes which caused problems. Wireless transmission was impressive as it allowed the user and tester a lot of freedom to move. If the visual test rig has to be moved or a test needed to be performed in a different venue, the wireless capability allowed for the necessary portability.

10.1.2 Goggle Negatives

The electrode placement was fixed within the frame of the goggles. For some users this was not a problem as the electrode position was correct for their faces. Other users might have struggled to get good results as the goggles were not able to adjust to a different facial geometry.

The goggles that were selected in this application were dirt biking goggles which are designed to withstand the force of high speed projectiles. The goggles were however, a little bulky and restricted peripheral vision slightly.

10.2 DC Slow Potential Drift Reduction

The drift phenomenon was very much active during the testing process. The method chosen to eradicate this drift to make sure that the signal stayed in range and did not saturate the operational amplifiers was to control it with a potentiometer. This component added a positive or negative DC component to the signal to neutralise the effect of the drift DC potential.

This method worked adequately; as once the DC signal was neutralised you could perform a test for a few minutes without having to worry about any further disturbance. However, occasionally the signal would continue to drift during the test and reach the operational amplifier limits. When the circuit limits are reached, no amount of post processing can then recapture the signal.

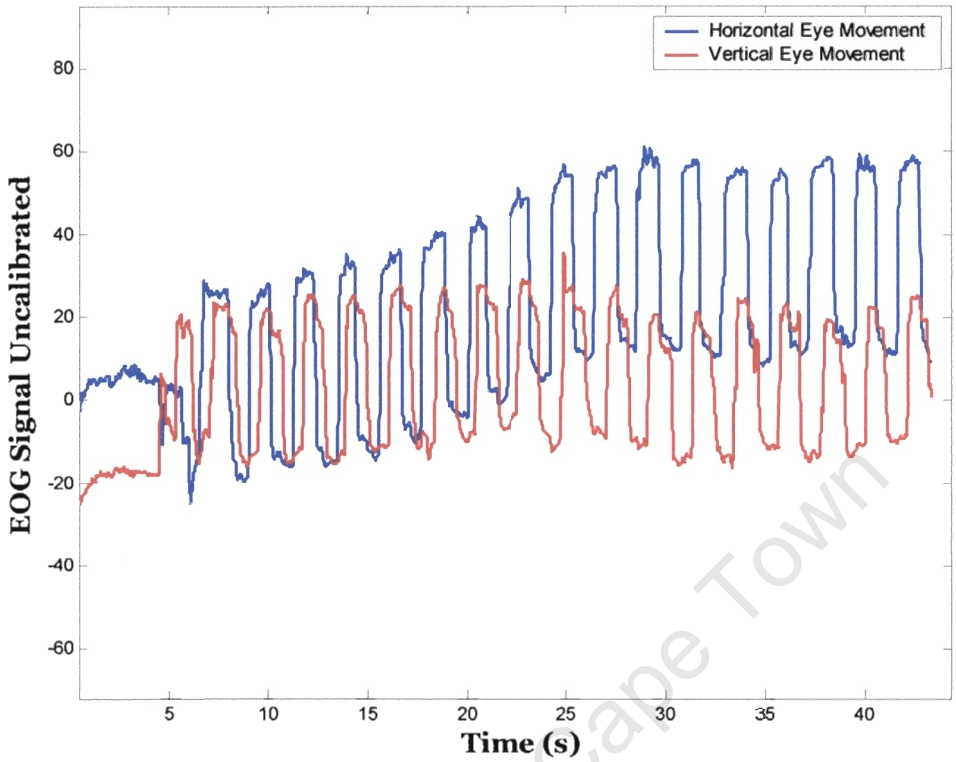

Figure 10.3: Shown above is data from an opposite corners test, which exhibits traits of the slow moving DC drift potential in the horizontal eye movement signal.

In the diagram above, it can be seen that the signal was properly calibrated at the start of the test. During the test however, the DC potential drift can be observed in the horizontal eye movement reading. In this case it levels out after 25s, but in some cases the drift continues to increase and can reach the operational amplifier limits.

10.3 Wireless Transmission

The wireless component of the board was one of the unique identifiers of this project. It provided the means for the project to fully reach its goal by implementing hassle free data transmission. The medium used was a 2.4 GHz transceiver which had a line of sight range of 10m.

For applications that were within 10m as in this project, the MC13192 wireless transceiver worked well. The requirements of the system were unchallenging for the wireless hardware and it coped comfortably with the 6.440 kbps data rate required.

High frequency signals are known to be weak at penetrating solid objects such as walls. It should be noted that this case was no exception. This 2.4 GHz transceiver worked best in line of sight conditions, with walls, desks and people being a hindrance to data transmission.

10.4 Microcontroller Performance

At the heart of all the data transmission were two MC9S08 microcontrollers. These components were responsible for interfacing analog circuitry, wireless components, parallel and serial transmission. These MCUs were used well within their limits and their performance was adequate to the needs of the project.

10.5 Electro-Oculographic Recordings

The final product after capture, processing, wireless transmission, reception, serial transmission and post processing is the EOG recording. The integrity of this recording is the litmus test of whether all the steps in the chain have functioned properly and whether the overall design works.

The following diagram shows the results of an SEMT random in position and time. The graph depicts horizontal and vertical eye movement with the visual stimuli (LEDs) firing times indicated by the blue line.

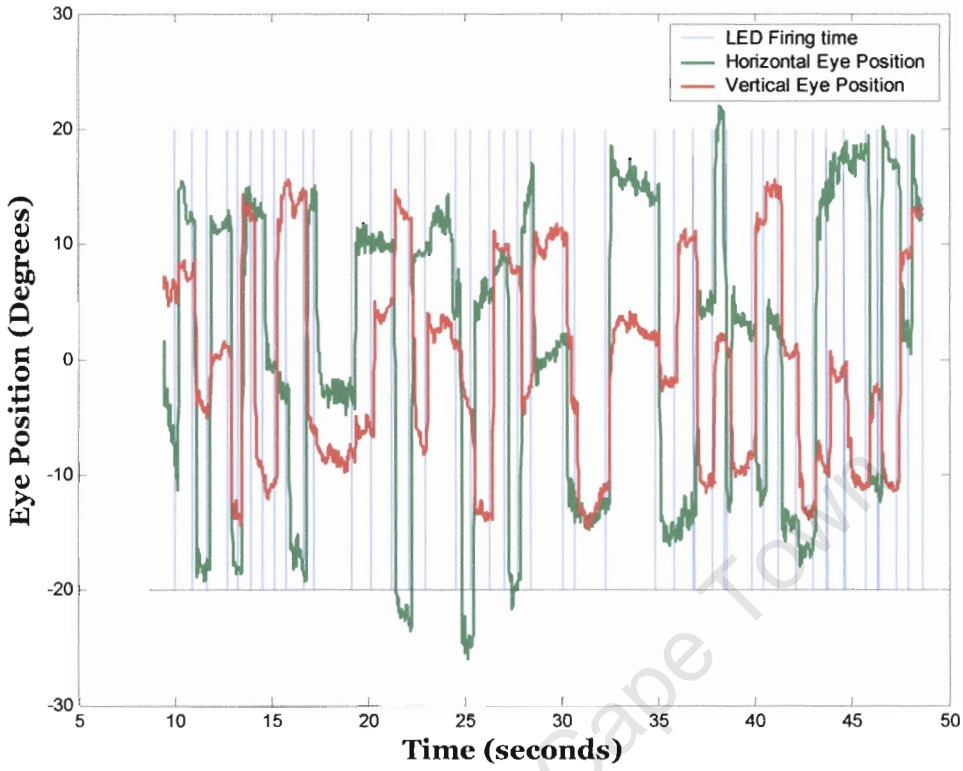

Figure 10.4: View of a 50 second SEMT showing the visual stimulus firing time, horizontal and vertical eye movement

As this is a zoomed out view, little technical information can be seen from this graph, but it gives an overview of what the signal looks like. The blue lines indicate the exact time that the visual stimulus changes position, the red and green lines indicate the horizontal and vertical movement of the eyes in response to these changes in visual stimulus position. This graph gives us information pertaining to saccadic speed, latency and overshoot in horizontal and vertical eye movement.

In the next diagram, a closer view is taken of the above graph over the time of **t=36** to **38s.** This enables us to get a better view of how we can ascertain the variables mentioned in the previous paragraph.

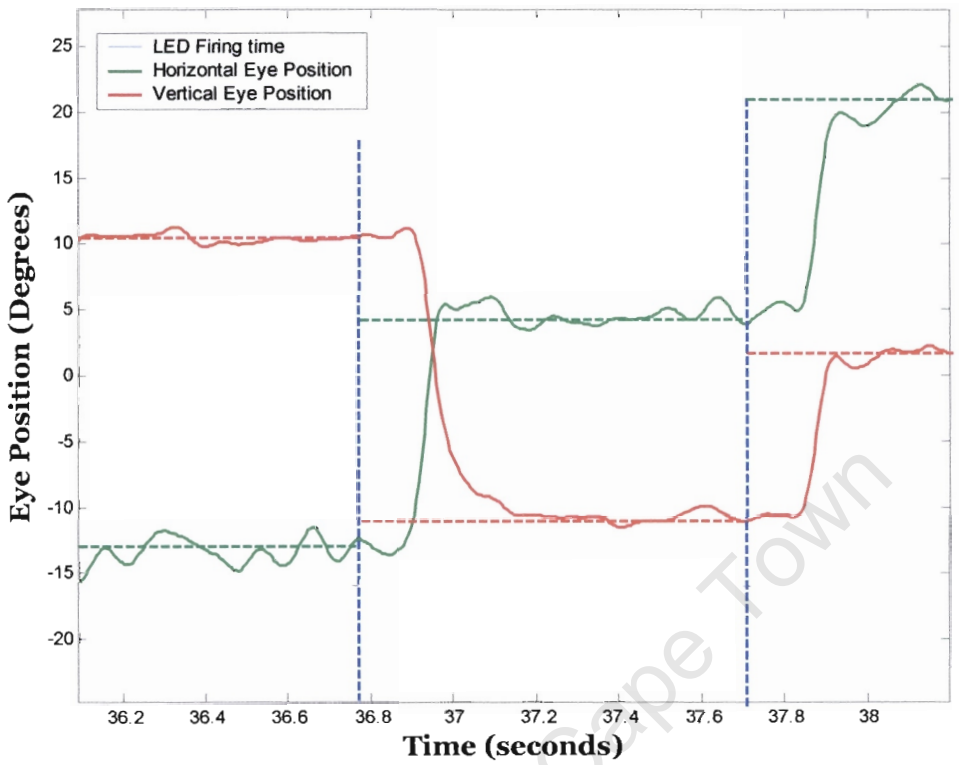

Figure 10.5: A zoomed in view of figure 10.4, the dotted blue lines depict the Visual Stimulus Firing Time, and horizontal and vertical eye movements are shown in green and red respectively.

When a new LED is fired, the visual stimulus changes (timing indicated by the blue line), as expected we notice that the eyes move into a new position. We also notice that before this movement, there is a delay. This delay is called the *saccadic latency*, and it marks the time that the brain and oculomotor system take to respond to a stimulus. This graph also shows the overall dynamic behaviour of the eye, or its *transfer function*.

It is through analysis of this transfer function, that we can extract the data that we want. In figure 10.6, we show a close up view of one of these transfer functions which allows us to make an accurate model.

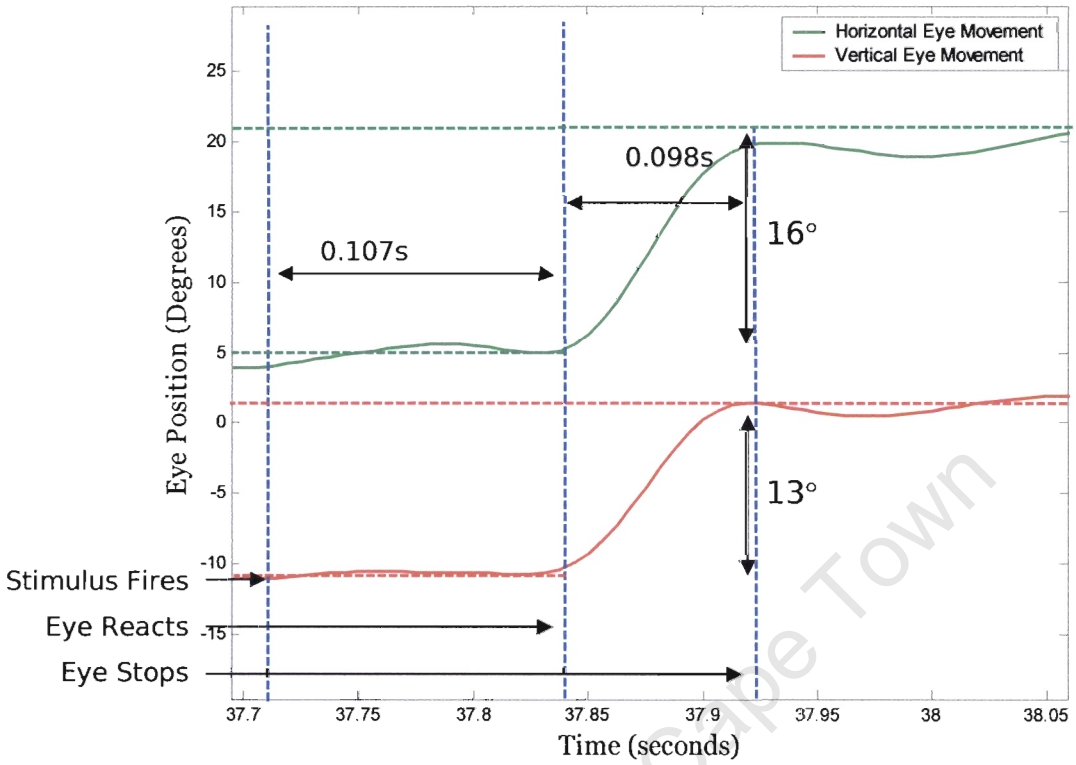

Figure 10.6: This diagram shows the horizontal and vertical transfer functions of the eye during a complete saccadic visual stimulus task.

The plot above shows a single horizontal and vertical eye reaction to a visual stimulus. At the leftmost blue line an LED is fired, this stimulus triggers the peripheral vision into transmitting the information to the visual cortex. The response occurs at the next blue line when the oculomotor system begins to move the eye. At the third blue line, the eye has reached its new position and remains there. The movement made in the horizontal and vertical directions are 16° and 13° respectively.

From figure 10.6, the following information pertaining to the oculomotor system can be extracted:

10.5.1 Saccadic Latency

When a visual stimulus is alerted in the peripheral vision of the human vision system, the information is transmitted along a neural pathway to the visual cortex and brain in order to make a decision. When this decision is made, another neural signal is used to generate a pulse that triggers the muscles in the eye in order to a saccadic eye movement which is signalled by eye velocities greater than 30°/s. This time delay is evident in the graph as the time difference between the two leftmost blue lines.

10.5.2 Ocular Overshoot and Undershoot

Ocular overshoot and undershoot pertains to eye movement accuracy. When the brain instructs the eye to move to a new position, the point at which the eye moves to is subject to an accuracy analysis. This analysis tells us if the eye has travelled too far (overshoot) or not far enough (undershoot).

It can be noted in figure 10.6 that the horizontal eye motion seems to exhibit an amount of undershoot. This phenomenon occurs when the eye reaches a peak that is lower than the setpoint. In this case this phenomenon is isolated, as in figure 10.5 we see the horizontal eye behaving without undershoot.

10.5.3 Peak Eye Velocity

Peak Eye Velocity is gained by looking at the differential of the eye position/time curve. A look at this graph gives us the information we need in order to compute the eye speed at any given time during the test. The maximum values are determined by the peaks and troughs of this graph. The Eye Velocity curve of figure 10.6 is shown below.

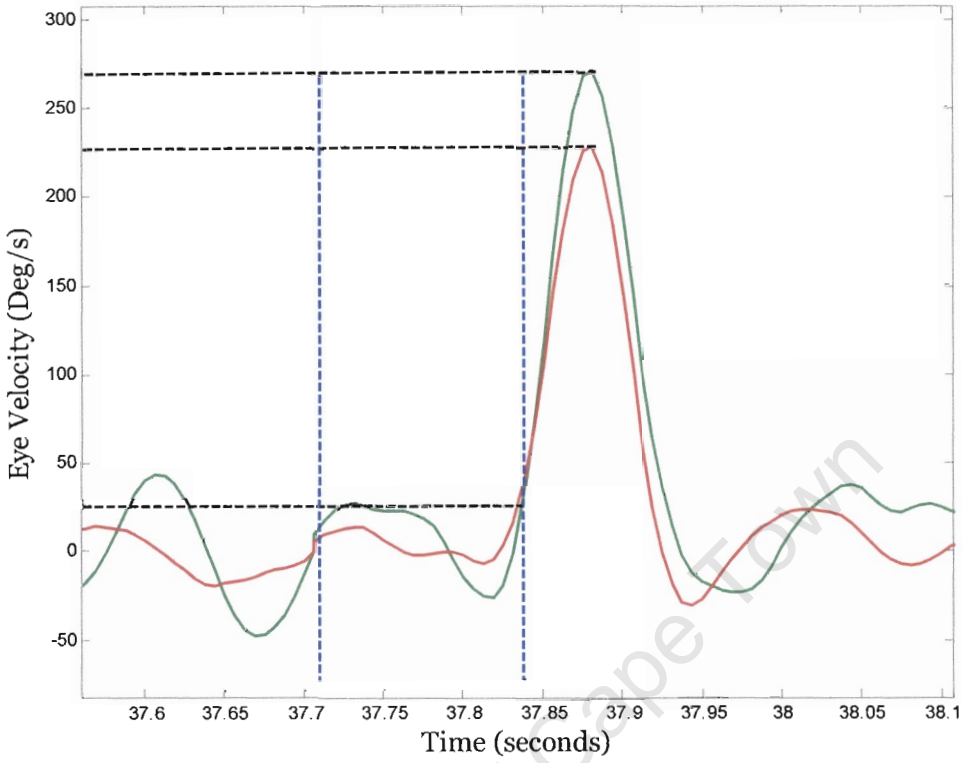

Figure 10.7: This graph shows the first derivative of the graph shown in figure 10.6. It shows the velocity of the eye during a saccadic eye movement.

The graph above shows us the eye velocity during the featured saccade in figure 10.6. It is clear to see where the peak eye velocity occurs during that saccade. In this case the maximum horizontal and vertical velocities are 271°/s and 227°/s respectively. The maximum velocity during the whole test was 505°/s.

11 CONCLUSIONS

After numerous tests were performed, each designed to test for weaknesses within the system; the following conclusions were made about the design project.

11.1 Electrode Housing Suitability

The EOG goggles worked well for the subjects that were tested. Provided that the goggles fitted well, we obtained good results. The important point is that there was some flexibility within the goggle frames. The plastic used in the frame is designed for comfort while dirt biking, so we found the frame very easy to adapt to a new face. This allowed for the slight variances in facial geometry without any compromises in signal quality.

The nature of the EOG signal is that is can be recalibrated if the electrodes are not in exactly the right position. Due to foreknowledge of angles of saccadic movements, we can use these angles in order to calibrate the readings obtained. This allows us to extract meaningful data even when the electrodes are not able to be placed in ideal positions.

11.2 Drift Reduction

Drift reduction was always going to be the biggest analog circuitry concern. In order to negate the effect of the random DC signal, a system of summing operational amplifiers was used to manually neutralise the DC Drift. These inputs were tweaked before testing to place the EOG signal within set operating limits of the operational amplifiers such that they did not saturate during testing.

This system did not work well for three reasons:

- The DC drift would sometimes continue to drift after calibration, and during testing, you could find that the signal has drifted out of the operating range.
- The potentiometers are often difficult to exactly calibrate as you might have a swing of 6.6V and when trying to add a small voltage of 0.1V, it can be difficult to achieve that on a single turn potentiometer.
- It is also difficult to adjust a potentiometer while the circuit is mounted on the goggles which somebody is wearing.

The result of these disadvantages meant that performing a test much longer than two minutes, could leave the tester facing the uncertainty of receiving null data for the latter part of the test.

11.3 Wireless Transmission

In order to evaluate the effectiveness of the wireless transmission medium, the important aspects to investigate in this project were data rate, range and circuit design considerations. These are discussed below:

11.3.1 Data Rate

The wireless transmission system was over designed from a data rate point of view. The MC13192 can transmit at a data rate of 250 kbps, whereas this application took 161 samples per second and therefore only demanded 6.44 kbps. This enabled the wireless module to run well within its limits.

11.3.2 Range

The power output of the MC13192 is largely dependent on whether the microstrip impedances on the output ports have been set correctly. In this case, the board used was 1.4mm thick as opposed to the thinner boards used in the development kit. This thickness discrepancy changed the capacitance to the ground plane which raised the impedance of the tracks. This increased output impedance caused the output power to suffer as a result. The range achievable was 10m.

11.3.3 Circuit Design Considerations

The MC13192 is a very small component. It is a 32 pin device which measures 5x5 mm. This compactness makes for a very neat circuit design, allowing for a desirable reduction in the overall circuit board size.

The small component design makes hand soldering impossible. The pads are located beneath the chip and are 0.3mm in width. It is necessary to have these components machine soldered onto the circuit board in order to ensure accuracy.

11.4 Microcontroller Performance

The Freescale MC9S08 microcontroller was programmed through Metrowerks Code Warrior in C using a BDM Multilink programmer.

The MC9S08 microcontrollers were used for

- A/D conversion of the EOG signal
- Time stamping the EOG signal
- Parallel communications with the LED control circuitry

- Serial (SCI, SPI) communications with the MC13192 components and via the serial port to the PC.

All these functions were carried out without any difficulties. It must be noted, however that the A/D conversion voltage range of the microcontroller must not be greater than the range of the supply.

11.5 High Level Software Analysis

Matlab was used to post process the gathered EOG data. It has the necessary high level functionality to import a text file of data and convert it into a matrix of numbers. It also has all of the complex mathematical toolboxes to perform the following necessary functions:

- High and Low pass Filtering
- Matrix Manipulation
- Calculus Operations

These toolboxes helped us to extract all of the data needed. The plot function gives us a visual interpretation of the data, which is how many of the graphs in this text are generated.

11.6 Electro-Oculographic Recording

In order to fully evaluate the results obtained by the EOG system, we have to compare them to previous models that have been published. The main parameters that define the human oculomotor system are saccadic latency and eye velocity. Provided that our readings of these parameters are in the same range as previous published results, we can assume the test to be an adequate representation of dynamic ocular motion.

In all of the listed literature, the test that posed the most similar resemblance to the test that was performed in this study was that of [25]. In this study, a test called the baseline saccadic test is very similar in nature to the one used in the EOG project. The baseline saccadic test entails using a small, square target that includes a series of positions within a ±13° range. A visual stimulus is triggered at each of these positions randomly which generates the saccadic eye movement at unpredictable times within 1.5 seconds. The subject used in this test is similar in age and gender and so similar results are expected between the two.

11.6.1 Saccadic Latency

The test in [25] measured values for the saccadic latency. The result of the test in [25] is that the mean for the saccadic latency with movements of ±13° was **0.972s**. In the test performed in this project we recorded a mean saccadic latency of **0.983s.**

The similarity of the testing and in the two sets of results seems to indicate a good correlation between the saccadic latency values obtained using the wireless EOG results in this project and the results obtained in [25] using an infrared eye tracker.

11.6.2 Peak Velocity

The graph below depicts a relationship between the peak velocities that can be expected from various saccadic amplitudes. In our test, it can be noted that the average peak velocity measured during an 18° saccade was 467.6°/s. The average as indicated by the graph should be about 400°/s. During the 9° saccadic tests,

the mean peak velocity was found to be 248.57°/s, where the graph indicates that a mean of 260°/s should be expected.

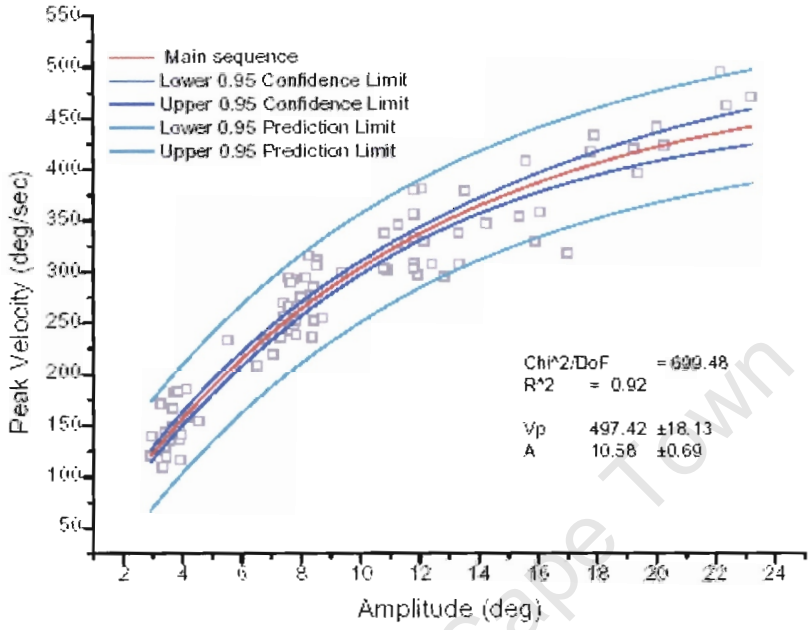

Figure 11.1: The relationship between peak velocity and saccadic amplitude and the upper and lower bounds of acceptable variability [25].

As these values are within the 0.95 prediction limits, we can deduct that our readings are consistent with findings from the study in [25].

12 RECOMMENDATIONS

Based on the conclusions in chapter 11, the following recommendations are made.

12.1 Electrode Housing

The EOG goggles were successful in making the EOG design hassle free and convenient to use. They provided a good, solid platform to hold the electrodes in place which eliminated any danger of the electrodes becoming unstable and/or falling off.

In a future project, other methods of housing the electrodes could include using a scrum cap or another more discreet pair of eyewear.

12.2 DC Drift Reduction

In order to eliminate the problems of DC drift, the best solution would be to automate the DC drift reduction process with a feedback loop. This feedback loop would seek to adjust the analog parameters of the circuit depending on the output signal. An example of the control loop is seen below:

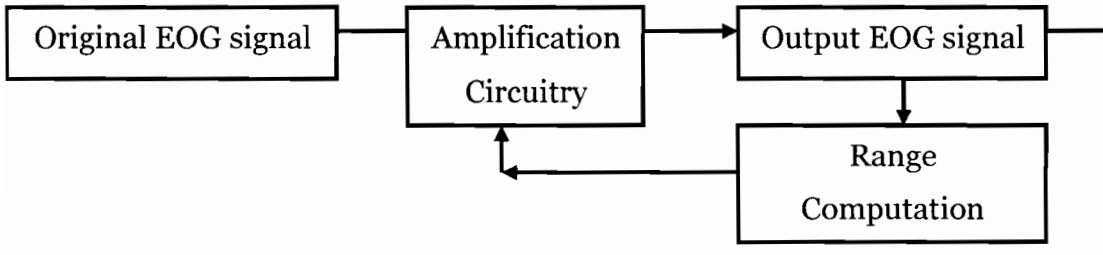

Figure 12.1: An example of the feedback loop that could correct the analog circuitry to ensure the correct range of the output EOG signal.

The microcontroller would be used to assess the range of the output EOG signal. Depending on this value, a range computation would be calculated and inputted into a series of digital potentiometers which would then affect the analog circuit.

12.3 Wireless Data Transmission and Microcontroller

In order to increase efficiency and reduce the programming required, a microcontroller and wireless module combination should be investigated. Having separate components increases complexity as a communication path needs to be set up between them. This adds work both in circuit design and programming.

Nordic semiconductor offers a 2.4 GHz wireless transceiver and microcontroller unit in one package. The microcontroller does not offer the wide range of functionality as a Freescale MC9S08, but the EOG application does not require advanced features. This modification would advance the transmit and receive circuit in both its compactness and ease of use.

12.4 High Level Software Analysis

The ideal situation would be to be able to fully automate the analysis of the signal. After a test, you could run a program which then generates values for mean saccadic latency and peak velocity with their variance. Currently, each of these modules have been programmed, but a complete software package would be important to develop in the future.

This would also allow for a more objective platform of measurement from one subject to another. For example, if we were testing a cricket team, all of the values generated could be directly compared without any disparities caused by human error in the measurement.

12.5 Electro-Oculographic Recording System

In future development of this project, the ideal measurement scenario would be to create a small testing facility which would include the following:

- A small dark room with many small independently programmable lights which act as visual stimuli.
- A few different pairs of EOG housing goggles which allow for different sizes of subject.
- A central seating console for the subject to sit while being tested. The console would include functionality to keep the subject's head from moving.
- A high level computer program that can set any of the test parameters and perform full data analysis after a test.

This facility would provide the means to create a professional and very capable means of visual testing. It could provide data relating to eye dynamics and eye movement accuracy. This could be the diagnostic means needed in order to fully evaluate the effect of sports vision training.

By providing information about the strengths and weaknesses of a player's visual system, this diagnostic information could also provide the necessary direction for a visual coach to pursue in a player's development.

13 REFERENCES

1. http://butler.cc.tut.fi/~malmivuo/bem/bembook/28/28.htm
2. Young LR, Sheena D (1988): Eye movement measurement techniques. In *Encyclopaedia of Medical Devices and Instrumentation*, ed. JG Webster, pp. 1259-9, John Wiley, New York
3. Analog Devices Datasheet, AD620 Instrumentation Amplifier
4. EOG Standards by ISCEV, www.ISCEV.org
5. Joseph J. Teccea,*, Linen J. Pokb, Michael R. Consiglioc, Jennifer L. O'Neild. A novel, portable eye tracking system for use in schizophrenia research. Attention Impairment in Electro-Oculographic control of Computer Functions. ISSC 2004, Belfast, June 30-July 2.
6. J.C. Corby, W.T. Roth and B.S. Kopell, Prevalence and Methods of Control of the Cephalic Skin Potential EEG Artefact.
7. J.M. Siegel, M.B. Sterman and S. Ross, Physiology & Behaviour, Vol.23, pp. 411-413. Automatic Detection and Operant Reinforcement of Slow Potential Shifts.
8. M.J. Coughlin, T.R.H. Cutmore, T.J. Hine. Automated Eye Tracking System Calibration using Artificial Neural Networks. Journal of Computer Methods and Programs in Biomedicine, www.intl.elsevierhealth.com/journals/cmpb.
9. J.S. Babcock and J.B. Pelz, Building a Lightweight Eyetracking Headgear. Rochester Institute of Technology.
10. J.S. Babcock, J.B. Pelz, The Wearable Eye Tracker: A Tool for the Study of High-Level Visual tasks, Rochester Institute of Technology.
11. Palmer, S.E. Vision Science Photons to Phenomenology. Cambridge, MA: MIT Press.
12. K. Hyoki, M. Shigeta, N Tsuno, Y Kawamuro, T. Kinoshita. Quantitative Electro-Oculography and Electro-Encephalography as Indices of Alertness. Electroencephalography and Clinical Neurophysiology 106 (1998) 213-219.

13. D. Melcher, Eileen Kowler, Visual Scene Memory and the Guidance of Saccadic Eye Movements, Vision Research 41 (2001) 3597-3611.
14. C. Martin, L. Schovanec, Muscle Mechanics and Dynamics of Ocular Motion, Journal of Mathematical Systems, Estimation and Control, Vol.8, No.2, 1998, pp.1-15.
15. L. Paninski, M. J. Hawken, Stochastic Optimal Control and the Human Oculomotor System, Neurocomputing, 38-40 (2001), pp. 1511-1517.
16. R.C. Miall, G.Z. Reckess, The Cerebellum and the Timing of Coordinated Eye and Hand Tracking, Brain and Cognition 48, pp. 212-226 (2002).
17. L. De Gennaro, M. Ferrara, L. Urbani, M. Bertini, Oculomotor Impairment after One Night Total Sleep Deprivation: a dissociation between measures of speed and accuracy, Clinical Neurophysiology 111 (2000), 1771-1778.
18. L. De Gennaro, M. Ferrara, L. Urbani, M. Bertini, Visual Search Performance across 40h of Continuous Wakefulness: Measures of Speed and Accuracy and relation with Oculomotor Performance, Physiology and Behaviour 74 (2001), 197-204.
19. M.S. Salman, J.A. Sharpe, M. Eizenman, L. Lillakas, C. Westall, T. To, M. Dennis, M.J. Steinbach, Saccades in Children, Vision Research (2006), pp. 1432-1439.
20. J.J. Clark, Spatial Attention and Latencies of Saccadic Eye Movements, Vision Research 39 (1999), pp. 585-602.
21. L.A. Dickov, J.D. Morrison, Effects of Uncertainty and Target Displacement on the Latency of Express Saccades in Man, Vision Research 46 (2006), pp. 2505-2512.
22. R. Walker, M. Husain, T.L. Hodgson, J. Harrison and C. Kennard, Saccadic Eye Movement and Working Memory Deficits following damage to Human Prefrontal Cortex, Neuropsychologia, Vol. 36, No. 11, pp.1141-1159, 1998.
23. Keith Holland, The Science of Behavioural Optometry.
24. By R.J. Babu. A Study of Saccade Dynamics and Adaptation in Athletes and Non-Athletes, Master's thesis in Vision Science, Waterloo, Ontario, Canada, 2004.

25. B Fischer, S. Everling, The Antisaccade: a Review of Basic Research and Clinical Studies, Neuropsychologia, Vol 36, No. 9, pp.885-899, 1998.
26. R. Barea, L. Boquette, M Mazo, E. Lopez, L.M. Bergasa. Electro-Oculographic Guidance of a Wheelchair using Eye Movements Codification. University of Alcala, Madrid, Spain. www.depeca.alcahala.es/personal/barea.
27. M. Brysbaert, D. Drieghe, F. Vitu. Word Skipping: Implications for Theories of Eye Movement Control in Reading. Royal Holloway, University of London, Ghent University, CNRS, Marseille, France.
28. Kluka, D.A. (1991). Visual Skills: Considerations in Learning Motor Skills for Sport. ASAHPERD Journal, 14(1), pp. 41-43.
29. D. Knudson (Baylor University), D. Kluka (University of Central Oklahoma), The impact of Vision and Vision Training on Sport Performance.
30. Shahied Taliep, PhD Dissertation, 2005, University of Cape Town
31. www.wikipedia.com
32. Fundamentals of Physics. By Halliday, Resnick, Walker.
33. Simple Media Access Controller. By Freescale.
34. MC13192 Reference Manual. By Freescale
35. MC13192 Data Sheet. By Freescale
36. Sensor Applications Reference Design. By Freescale.

A APPENDICES

A.1 EOG Circuit Schematic

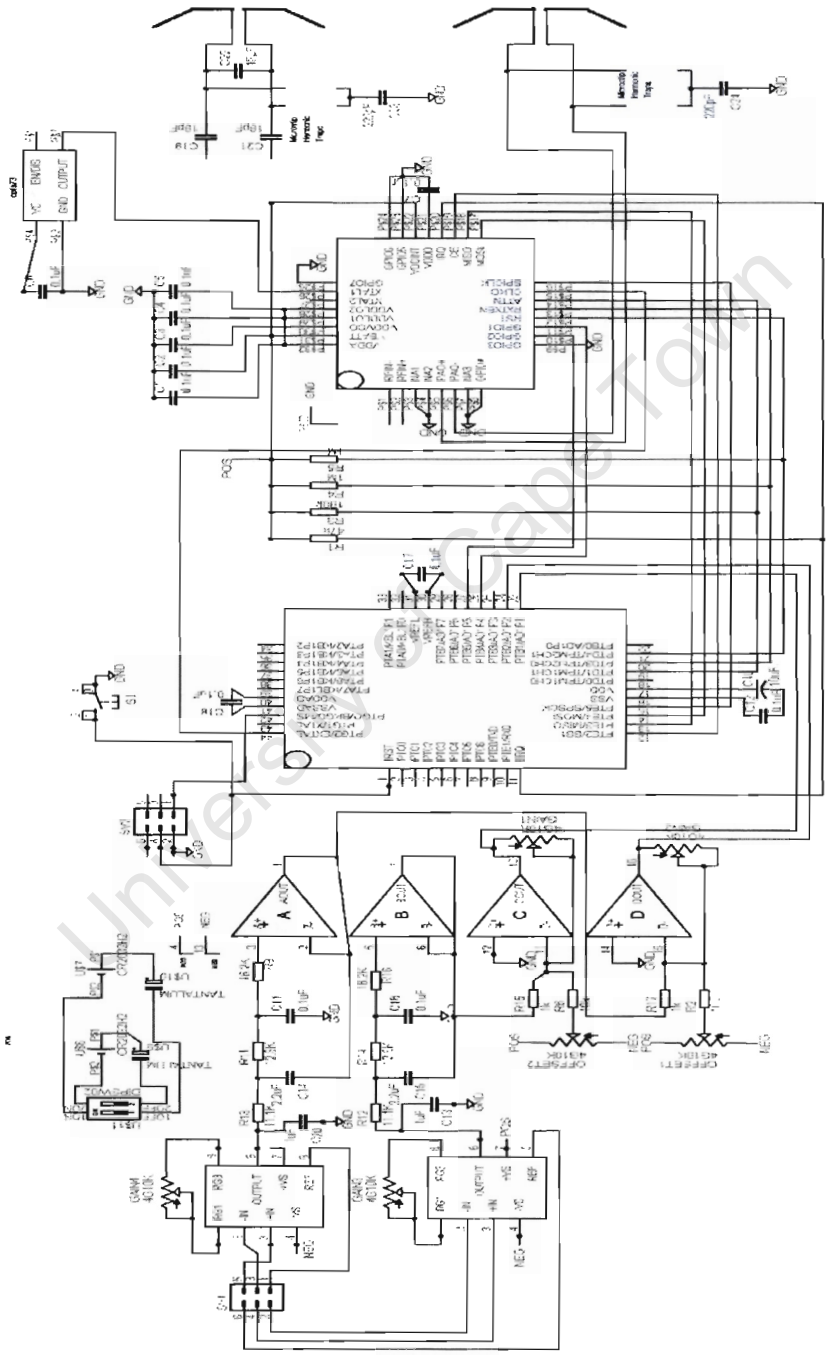

A.2 Matlab Code

A.2.1 EOG Analysis

```
function T = EOGAnalyse(Y)
OrigY1=Y;
Y = LPF(Y,16);
r = length(Y);
SecDerivStaticPoints = 0;
SecDerivY = 0;
SumValueStatic =0;
NumStaticPoints=0;
MaxStaticValue =0;
for i = 1 : r-1
   DerivY(i) = Y(i+1)-Y(i);
end

r = length(DerivY);

for i = 1 : r-1
   SecDerivY(i) = DerivY(i+1)-DerivY(i);
end

r = length(SecDerivY);

for i = 17 : r-1
   if (SecDerivY(i+1)*SecDerivY(i)) < 0
      SecDerivStaticPoints(i) = DerivY(i+1);
      if DerivY(i+1)>MaxStaticValue
         MaxStaticValue = DerivY(i+1);
      end
   end
end

lastpoint=1;
```

```
laststatic=1;
maxfound=0;
r= 1: length(DerivY);

for i = 1 :length(SecDerivStaticPoints)

  if ((abs(SecDerivStaticPoints(i))<=0.25*MaxStaticValue)&(SecDerivStaticPoints(i)~=0))
    laststatic = i;
    if maxfound == 1
      maxfound=0;
      lastpoint = i;
    end
  end

  if abs(SecDerivStaticPoints(i))>0.25*MaxStaticValue
    TobeLPF=0;
    for j = lastpoint : laststatic
      TobeLPF(j-lastpoint+1)=DerivY(j);
    end
    TobeLPF = LPF(TobeLPF,512);
    for j = lastpoint : laststatic
      DerivY(j)=0;%TobeLPF(j-lastpoint+1);
    end
    maxfound=1;
  end
end

r= 1: length(DerivY);
%plot(r,DerivY,'r');
OrigY(1)=0;
OrigY(2)=0;

for i = 2 : length(DerivY)
  OrigY(i) = OrigY(i-1)+DerivY(i);
end

r = 1 : length(OrigY1);
subplot(3,1,1);
```

```
plot (r,OrigY1,'c');

r = 1 : length(Y);
subplot(3,1,2);
plot (r,Y,'b');

r = 1 : length(OrigY);
subplot(3,1,3);
plot (r,OrigY,'r');
end
```

A.2.2 Time Calibration

```
sumtime =0;
prednewtotaltime=0;

for i = 2 : length(predtotaltime)-1
  prednewtotaltime(i)=predtotaltime(i)+sumtime;
   if (predtotaltime(i+1)-predtotaltime(i))<0
      sumtime = sumtime + predtotaltime(i)-predtotaltime(i+1);
   end
end
```

A.2.3 Low Pass Filter

```
function T = LPF(Y,N)
p = 0:16;
for n = 0 : N
   w(n+1) = 0.50-0.50*cos(2*pi*n/N);
end

for n = 1 : length(Y)
sum = 0;
p=0;
  for k = n-N : n
```

```
  if k > 0
    if n-k>=0
    sum= sum + Y(k)*w(n-k+1);
    end
   end
 end
 y(n+1) = sum*2/N;
end

for i = N/2+1 :length(y)
  y(i-N/2)=y(i);
end

y(1)=y(2);
T=y;
End
```

A.2.4 LED Calibration

```
derLEDs=0;
for i = 1 : length(LEDs)-1
  derLEDs(i)=LEDs(i+1)-LEDs(i);
end
derLEDs=abs(derLEDs);

for i = 1 : length(derLEDs)
  if (derLEDs(i)~=0)
    derLEDs(i)=1;
  end
end

derLEDs=(derLEDs-0.5)*40;

for i = 1 : length(derLEDs)
  if (derLEDs(i)==-20)
    derLEDs(i)=0;
```

```
  end
end
```

A.3 Visual Basic Code

```
Dim test As String
Dim Ocheck, XPrev, YPrev As Integer
Dim fso, txtfile

Private Sub Form_Load()

  Set fso = CreateObject("Scripting.FileSystemObject")
  Set txtfile = fso.CreateTextFile("c:\test.txt", True)
  txtfile.writeline ("Electro-Oculography Data. ") ' Write a line.
  Set txtfile = fso.CreateTextFile("c:\testfile.txt", True)

End Sub

Private Sub CalibrateBegin_Click()
CalibrateBegin.Enabled = False
CalibrationEnd.Enabled = True
Call Openport
test = EOGData.Input
If (Mid(test, 1, 1) = "x") Then
  XEOGValue.Text = Str(Asc(Mid(test, 2, 1)))
  X = Asc(Mid(test, 2, 1))
End If

If (Mid(test, 3, 1) = "y") Then
  YEOGValue.Text = Str(Asc(Mid(test, 4, 1)))
  Y = Asc(Mid(test, 4, 1))
End If
Call Drawpath(XPrev * 24 + 115, YPrev * 20 + 210, vbBlack)
Call Drawpath(X * 24 + 115, Y * 20 + 210, vbWhite)
XPrev = X
```

```
YPrev = Y
End Sub

Private Sub OpenEOGport()
EOGData.CommPort = 1
EOGData.PortOpen = True
EOGData.Settings = "38400,N,8,1"
EOGData.InputLen = 7
End Sub

Private Sub CloseEOGport()
EOGData.PortOpen = False
End Sub

Private Sub CalibrationEnd_Click()
Call Closeport
CalibrateBegin.Enabled = True
CalibrationEnd.Enabled = False
End Sub

Private Sub Drawpath(X, Y, Colour)
Dim i As Integer
  For i = 0 To 1
    For j = 0 To 1
    Picture1.PSet (X + i, Y + j), Colour
    Next j
  Next i
End Sub


Sub OpenFile(filename As String)
  Dim fso, txtfile
  Set fso = CreateObject("Scripting.FileSystemObject")
  Set txtfile = fso.CreateTextFile("c:\horizontalthenvertical.txt", True)
  txtfile.writeline ("Electro-Oculography Data. ") ' Write a line.
End Sub

Private Sub EOGData_OnComm()
```

```
test = EOGData.Input

If (Len(test) = 7) Then
 If InStr(test, "x") > 1 Then
  newtest = "      "
  intermed = Mid(test, 1, InStr(test, "x") - 1)
  Mid(newtest, Len(test) - InStr(test, "x") + 2, InStr(test, "x") - 1) = intermed
  intermed = Mid(test, InStr(test, "x"), Len(test) - InStr(test, "x") + 1)
  Mid(newtest, 1) = intermed
  test = newtest
  'test = Replace(test, Mid(Len(test), 1, 1), Mid(test, 1, InStr(test, "x")))
  'test = Replace(test, Mid(test, 1, 1), "", 1, InStr(test, "x") + 1)
 End If

 If (Mid(test, 1, 1) = "x") Then
  If (Mid(test, 3, 1) = "y") Then

   txtfile.write (" ")
   txtfile.write (Str(Asc(Mid(test, 2, 1))))
   txtfile.write (" ")
   X = Asc(Mid(test, 2, 1))

   txtfile.write (Str(Asc(Mid(test, 4, 1))))
   txtfile.write (" ")
   Y = Asc(Mid(test, 4, 1))

   txtfile.write (Str(Asc(Mid(test, 5, 1))))
   txtfile.write (" ")
   txtfile.write (Str(Asc(Mid(test, 6, 1))))
   txtfile.write (" ")
   txtfile.writeline (Str(Asc(Mid(test, 7, 1))))
   End If
  End If
End If
End Sub

Private Sub NewSubjectOK_Click()
NewSubjectOK.Visible = False
```

```
SubjectName.Visible = False
NewSubjectFrame.Visible = False
Timer1.Enabled = True
Call OpenEOGport
End Sub

Private Sub RuntestEnd_Click()
RuntestEnd.Enabled = False
StartTest.Enabled = True
Timer1.Enabled = False
Call CloseEOGport
End Sub

Private Sub StartTest_Click()
StartTest.Enabled = False
RuntestEnd.Enabled = True
NewSubjectOK.Visible = True
SubjectName.Visible = True
NewSubjectFrame.Visible = True
End Sub
End Sub
```

A.4 C Code

A.4.1 Receiver and Test Facility Control Code

```
#include <hidef.h> /* for EnableInterrupts macro */
#include "device_header.h"
#include "pub_def.h"
#include "simple_mac.h"
#include "mcu_hw_config.h"
#include "MC13192_hw_config.h"
#include "SCI.h"
#include "drivers.h"
#include "accelerometer.h"
```

```
#include "bootloader user api.h"
#include <MC9S08GT60.h> /* include peripheral declarations */

/* Global Variables */

  #define LEDBL   PTBD_PTBD7
  #define LEDML   PTAD_PTAD6
  #define LEDTL   PTAD_PTAD7
  #define LEDTM   PTCD_PTCD0
  #define LEDTR   PTCD_PTCD1
  #define LEDMR   PTCD_PTCD5
  #define LEDBR   PTCD_PTCD6
  #define LEDBM   PTGD_PTGD1

                #define PUSH_BUTTON1  PTAD_PTAD2
  #define PUSH_BUTTON2  PTAD_PTAD3
  #define PUSH_BUTTON3  PTAD_PTAD4
  #define PUSH_BUTTON4  PTAD_PTAD5
  #define LOW_POWER_WHILE() _asm wait
  #define INITIAL_STATE 0
  #define IDLE_STATE 1
  #define RECEIVER_ALWAYS_ON 2

typedef unsigned char   UINT8;     /*unsigned 8 bit definition */
typedef unsigned short  UINT16;    /*unsigned 16 bit definition*/
typedef unsigned long   UINT32;    /*unsigned 32 bit definition*/
typedef signed char     INT8;      /*signed 8 bit definition */
typedef short           INT16;     /*signed 16 bit definition*/
typedef long int        INT32;     /*signed 32 bit definition*/

int whattime = 0;

UINT8 gu8RTxMode;
INT8 gi8AppStatus = 0;

UINT8 gau8TxDataBuffer[16];
UINT8 gau8RxDataBuffer[16];
```

```
unsigned int totaldelay;
unsigned int currenttime;
int i;
int count1;
int LEDcurrent;
int randomdelay;
short delaytime;
unsigned int current_config[100];
int dog;
int randno =0;
int length;
int PrevLED;

 int  w; /* w[0] is MSB, w[1] is LSB */
 int i = 0x000F;
 int g = 0x000E;

int BL;
int ML;
int TL;
int TM;
int TR;
int MR;
int BR;
int BM;
int g;

tRxPacket gsRxPacket;

//////////////////////////////
/* note: Buad Rate = 38400 */
//////////////////////////////

/* Global Variables */
UINT8 gu8RTxMode;

UINT8 gau8TxDataBuffer[16];
UINT8 gau8RxDataBuffer[16];
```

```
tTxPacket gsTxPacket;
tRxPacket gsRxPacket;


void main(void)
{
////////////////////
/* Init routines   */
////////////////////

 MCUInit();
 MC13192Init();
 AppInit();
 SCIInit();

 MLMESetMC13192ClockRate(0);  /* Set initial Clk speed */

 BL = 0x0001; ML = 0x0002; TL = 0x0004; TM = 0x0008;
 TR = 0x0010; MR = 0x0020; BR = 0x0040; BM = 0x0080;

 PTBDD = 0xFF;

 PTAPE_PTAPE2 = 1;
 PTAPE_PTAPE3 = 1;
 PTAPE_PTAPE4 = 1;
 PTAPE_PTAPE5 = 1;

 PTADD_PTADD2 = 0;
 PTADD_PTADD3 = 0;
 PTADD_PTADD4 = 0;
 PTADD_PTADD5 = 0;

 PTADD_PTADD6 = 1;
 PTADD_PTADD7 = 1;
 PTCDD_PTCDD6 = 1;
 PTCDD_PTCDD5 = 1;
 PTCDD_PTCDD1 = 1;
 PTCDD_PTCDD0 = 1;
```

```
 PTGDD_PTGDD1 = 1;
 SOPT = 0x73;

 MLMEMC13192PAOutputAdjust(MAX_POWER);   //Set MAX power setting
 UseExternalClock();   /* switch clock sources from mcu to MC1319x CLKO*/

#ifdef BOOTLOADER_ENABLED
   boot_init();  /* Initialize the bootloader. */
#endif BOOTLOADER_ENABLED

#ifdef BOOTLOADER_ENABLED
   boot_call();  /* Check for user request to run bootloader. */
            /* App will not return, if Bootloader is requested. */
#endif BOOTLOADER_ENABLED

   gi8AppStatus = INITIAL_STATE;   /* Initial Mode */
   if (MLMESetChannelRequest(5) == SUCCESS) { /* Select channel here (0-15) */
          gi8AppStatus = RECEIVER_ALWAYS_ON;
   }

 for (;;){

 EnableInterrupts; /* enable interrupts */

 MC13192Init();

 delaytime = 0x0160;
 count1 = 52;
 PrevLED=BL;

 if (PUSH_BUTTON1 == 0) {
  for (;;){

    if (PrevLED == TL){
      LEDcurrent = BR;
    }
    if (PrevLED == BR){
      LEDcurrent = TR;
```

```
  }
  if (PrevLED == TR){
   LEDcurrent = BL;
  }
  if (PrevLED == BL){
   LEDcurrent = TL;
  }


  LEDBL = LEDcurrent & 0x0001;
  LEDML = (LEDcurrent >>1) & 0x0001;
  LEDTL = (LEDcurrent >>2) & 0x0001;
  LEDTM = (LEDcurrent >>3) & 0x0001;
  LEDTR = (LEDcurrent >>4) & 0x0001;
  LEDMR = (LEDcurrent >>5) & 0x0001;
  LEDBR = (LEDcurrent >>6) & 0x0001;
  LEDBM = (LEDcurrent >>7) & 0x0001;

  TPM1SC = 0x0F;
  TPM1CNTL = 0x00;
  totaldelay = 0xBFFF;

  do {
   RxAccel();
   } while (TPM1CNT <= totaldelay);
  PrevLED = LEDcurrent;
 }
}

if (PUSH_BUTTON2 == 0) {
 for (;;){

  randno = rand();
  randomdelay = rand();

  if ((randno>0)&(randno<=4096)){
   LEDcurrent = BL;
  }
```

```
if ((randno>4096)&(randno<=8192)){
 LEDcurrent = BM;
}
if ((randno>8192)&(randno<=12288)){
 LEDcurrent =  BR;
}
if ((randno>12288)&(randno<=16384)){
 LEDcurrent = TL;
}
if ((randno>16384)&(randno<=20480)){
 LEDcurrent = TM;
}
if ((randno>20480)&(randno<=24576)){
 LEDcurrent =  TR;
}
if ((randno>24567)&(randno<=28672)){
 LEDcurrent = ML;
}
if ((randno>28672)&(randno<=32768)){
 LEDcurrent =  MR;
}

LEDBL = LEDcurrent & 0x0001;
LEDML = (LEDcurrent >>1) & 0x0001;
LEDTL = (LEDcurrent >>2) & 0x0001;
LEDTM = (LEDcurrent >>3) & 0x0001;
LEDTR = (LEDcurrent >>4) & 0x0001;
LEDMR = (LEDcurrent >>5) & 0x0001;
LEDBR = (LEDcurrent >>6) & 0x0001;
LEDBM = (LEDcurrent >>7) & 0x0001;

TPM1SC = 0x0F;
TPM1CNTL = 0x00;
totaldelay = 0x7FFF+randomdelay;

do {
 RxAccel();
 } while (TPM1CNT <= totaldelay);
```

```
  }
 }


if (PUSH_BUTTON3 == 0) {
  count1 = 4;
  for (;;){
   corner_clockwise(0);

    for (i=0; i < count1; i++){
    LEDBL = current_config[i] & 0x0001;
    LEDML = (current_config[i] >>1) & 0x0001;
    LEDTL = (current_config[i] >>2) & 0x0001;
    LEDTM = (current_config[i] >>3) & 0x0001;
    LEDTR = (current_config[i] >>4) & 0x0001;
    LEDMR = (current_config[i] >>5) & 0x0001;
    LEDBR = (current_config[i] >>6) & 0x0001;
    LEDBM = (current_config[i] >>7) & 0x0001;

    delay(delaytime);}
  }
 }


if (PUSH_BUTTON4 == 0) {
  count1 = 8;
  for (;;){
   horizontal(0);
   vertical(4);

    for (i=0; i < count1; i++){
    LEDBL = current_config[i] & 0x0001;
    LEDML = (current_config[i] >>1) & 0x0001;
    LEDTL = (current_config[i] >>2) & 0x0001;
    LEDTM = (current_config[i] >>3) & 0x0001;
    LEDTR = (current_config[i] >>4) & 0x0001;
    LEDMR = (current_config[i] >>5) & 0x0001;
    LEDBR = (current_config[i] >>6) & 0x0001;
```

```
    LEDBM = (current_config[i] >>7) & 0x0001;

    delay(delaytime);}
  }
 }
}

}

/*****************************************************************
*  Function:    RX_accel
*  Parameters: none
*  Return:      none
*
*  This is the main thread of execution when no button is pressed
*  on reset.
*****************************************************************/
void RxAccel(void) {
    EnableInterrupts;

 /*****************************************************************
 *   RX_accel main loop
 *****************************************************************/

    switch (gi8AppStatus)
    {

      case IDLE_STATE:
        /*Switch to RECEIVER_ALWAYS_ON */
        gi8AppStatus = RECEIVER_ALWAYS_ON;
        break;

      case RECEIVER_ALWAYS_ON:
          MLMERXEnableRequest(&gsRxPacket, 0);
          LOW_POWER_WHILE();
        break;

      /* Should not get here. */
```

```
        default:
          gi8AppStatus = RECEIVER_ALWAYS_ON;
            }
}

*****************************************************************
*   Function:    MCPS_data_indication
*   Parameters: gsRxPacket_t
*   Return:      none
*
*   This is the callback function for when a valid packet has been
*   decoded by the radio.  The valid packet is passed to the app
*    via this MCPS_data_indication callback function.  All the data
*   resides in the gsRxPacket in this function but is also passed
*   back to the main via gsRxPacket in the main/RX_accel thread.
*   This routine is in the interrupt processing call stack.  It
*   is not recommended to call other radio functions here.
*****************************************************************/

void MCPSDataIndication(tRxPacket *gsRxPacket)
{

  /*
     * RX packet is in the global structure
   * gsRxPacket.dataLength and gsRxPacket.data
   */

  if (gsRxPacket->u8Status == SUCCESS)
  {

    /* Good Packet Received Check for proper x?y?z? data format */
    if ((gsRxPacket->pu8Data[0] == 'x') &&
      (gsRxPacket->pu8Data[2] == 'y'))
    {
        gau8RxDataBuffer[0] = gsRxPacket->pu8Data[0];
                              gau8RxDataBuffer[1] = gsRxPacket->pu8Data[1];
        gau8RxDataBuffer[2] = gsRxPacket->pu8Data[2];
        gau8RxDataBuffer[3] = gsRxPacket->pu8Data[3];
```

```
        gau8RxDataBuffer[4] = TPM1CNTH;
        gau8RxDataBuffer[5] = TPM1CNTL;
        gau8RxDataBuffer[6] = LEDcurrent;

        length = 7 ;
        LED3 ^= 1;
        SCITransmitArray(gau8RxDataBuffer, length);
    }
  }
}

void MLMEMC13192ResetIndication (void)
{
/* Not implemented. */
}
/*************************************************************
*  Function:    AppInit
*  Parameters: none
*  Return:      none
*
*  Sets up the initial hardware initialization for the app.
*************************************************************/

void AppInit(void)
{

 LED1DIR = 1;   /* Setup LED ports as outputs*/
 LED2DIR = 1;   /* Setup LED ports as outputs*/
 LED3DIR = 1;   /* Setup LED ports as outputs*/
 LED4DIR = 1;   /* Setup LED ports as outputs*/

 LED1 = LED_OFF;   /* Turn LEDs OFF */
 LED2 = LED_OFF;   /* Turn LEDs OFF */
 LED3 = LED_OFF;   /* Turn LEDs OFF */
 LED4 = LED_OFF;   /* Turn LEDs OFF */

 PB0PU = 1;    /* Pushbutton directions and pull-ups */
 PB0DIR = 0;
```

```
 PB1PU = 1;
 PB1DIR = 0;
 PB2PU = 1;
 PB2DIR = 0;
 PB3PU = 1;
 PB3DIR = 0;


  /* Initialize the packet. */
 gsTxPacket.u8DataLength = 0;   /* Initialize the gsTxPacket global */
 gsTxPacket.pu8Data = &gau8TxDataBuffer[0]; /* Set the pointer to point to the tx_buffer */

 gsRxPacket.u8MaxDataLength = 0;
 gsRxPacket.pu8Data = &gau8RxDataBuffer[0];
 gsRxPacket.u8MaxDataLength = 16;   /* Arbitrary, bigger than xXyYzZ format. */
 gsRxPacket.u8Status = 0;            /* initialize status to 0. */
}

/*************************************************************
*   Function:    delay
*   Parameters: 16-bit delay value
*   Return:      none
*
*   Simple delay loop.
*************************************************************/

void delay(INT16 count)
{
  INT16 i;
  for (i=0; i<count; i++);
}

int all_clockwise(int k){
 current_config[k] = BL;
 current_config[k+1] = ML;
 current_config[k+2] = TL;
 current_config[k+3] = TM;
 current_config[k+4] = TR;
```

```
 current_config[k+5] = MR;
 current_config[k+6] = BR;
 current_config[k+7] = BM;
}

int all_anticlockwise(int k){
 current_config[k] = BL;
 current_config[k+1] = BM;
 current_config[k+2] = BR;
 current_config[k+3] = MR;
 current_config[k+4] = TR;
 current_config[k+5] = TM;
 current_config[k+6] = TL;
 current_config[k+7] = ML;
}


int corner_clockwise(int k) {

 current_config[k] = BL;
 current_config[k+1] = TL;
 current_config[k+2] = TR;
 current_config[k+3] = BR;
}

int corner_anticlockwise(int k) {

 current_config[k] = BL;
 current_config[k+1] = BR;
 current_config[k+2] = TR;
 current_config[k+3] = TL;
}

int horizontal(int k){

 current_config[k] = ML;
 current_config[k+1] = MR;
 current_config[k+2] = ML;
```

```
 current_config[k+3] = MR;
}

int vertical(int k){

 current_config[k] = TM;
 current_config[k+1] = BM;
 current_config[k+2] = TM;
 current_config[k+3] = BM;
}
int random_sequence(int k){

 for (i=0;i<8;i++){

  randno = rand();

  if ((randno>0)&(randno<=4096)){
   current_config[k+i] = BL;
  }

  if ((randno>4096)&(randno<=8192)){
   current_config[k+i] = BM;
  }
  if ((randno>8192)&(randno<=12288)){
   current_config[k+i] = BR;
  }
  if ((randno>12288)&(randno<=16384)){
   current_config[k+i] = TL;
  }
  if ((randno>16384)&(randno<=20480)){
   current_config[k+i] = TM;
  }
  if ((randno>20480)&(randno<=24576)){
   current_config[k+i] = TR;
  }
  if ((randno>24567)&(randno<=28672)){
   current_config[k+i] = ML;
  }
```

```
  if ((randno>28672)&(randno<=32768)){
    current_config[k+i] = MR;
  }
 }
}
```

A.4.2 EOG Transmitter Code

```
#include <hidef.h> /* for EnableInterrupts macro */
#include <MC9S08GT16.h> /* include peripheral declarations */
#include <hidef.h> /* for EnableInterrupts macro */
#include "device_header.h"
#include "pub_def.h"
#include "simple_mac.h"
#include "simple_phy.h"
#include "mc13192_hw_config.h"
#include "MC13192_regs.h"
#include "drivers.h"
#include "main.h"
#include "SCI.h"
/* Global Variables */
#define IRQFLAG                IRQSC_IRQF
/*/define IRQACK()              IRQSC |= 0x04*/
#define IRQInit()              IRQSC = 0x14
#define IRQPinEnable()         IRQSC = 0x16

UINT8 gu8RTxMode;
UINT8 test8;

INT8 gi8AppStatus = 0;

UINT8 gau8TxDataBuffer[16];
UINT8 gau8RxDataBuffer[16];
tTxPacket gsTxPacket;
tRxPacket gsRxPacket;

void UseExternalClock() //use_external_clock()
```

```
{
  ICGC1 = 0x50;  /*
                  * 0b01010000
                  *  ||||||||__ Unimplemented
                  *    |||||||___ Unimplemented
                  *    ||||||____ Oscillator disabled when ICG is in
                  *  |||||    off mode
                  *    |||||
                  *    ||||+_____ FLL bypassed, external reference
                  *    |||_______ External Clock Requested
                  *    ||________ Osc configured for High Frequency
                  *    |_________ Unimplemented
                  */
  while (!ICGS1_ERCS)   /* Wait for external reference to be stable. */
    ;
  ICGC2_LOLRE = 1;
  ICGC2_MFD = 0x00;     /* Mult factor of 4. */
}
void GPIOInit()
{
  /*MC13192_RESET_PULLUP = 0;*/

  PTDDD_PTDDD1 = 1;
  PTDDD_PTDDD3 = 1;
  PTDDD_PTDDD4 = 1;
  PTEDD_PTEDD2 = 1;
  PTED_PTED2 = 1;
  MC13192_ATTN = 1;
  MC13192_RTXEN = 0;
  PTDD_PTDD4 = 0;  /* Do not initially reset MC13192 */

/*  MC13192_CE_PORT = 1;
  MC13192_ATTN_PORT = 1;
  MC13192_RTXEN_PORT = 1;
  MC13192_RESET_PORT = 1;*/

/*  MC13192_CE = 1;
  MC13192_ATTN = 1;
```

```
  MC13192_RTXEN = 0;
  MC13192_RESET = 0;  */            /* Do not initially reset MC13192 */

  #if defined (ANTENNA_SWITCH)
    MC13192_ANT_CTRL2_PORT = 1;      /* Output for antenna port RX */
    MC13192_ANT_CTRL_PORT = 1;       /* Output for antenna port TX */
    MC13192_ANT_CTRL2 = 1;          /* Signal to turn on RX antenna */
    MC13192_ANT_CTRL = 1;           /* Signal to turn on TX antenna */
  #endif

  #if defined (LNA)
    MC13192_LNA_CTRL = LNA_OFF;     /* Turn off the LNA out of reset */
    MC13192_LNA_CTRL_PORT  = 1;     /* Enable the port for OUTPUT */
  #endif

  #if defined (PA)
    MC13192_PA_CTRL = PA_OFF;       /* Turn off the PA out of Reset */
    MC13192_PA_CTRL_PORT = 1;       /* Enable the port for OUTPUT */
  #endif
}
void main(void) {

  UINT16 u16IrqReg =0;
  UINT8 u8AttnIrq = FALSE;
  UINT8 u8TimerHi, u8TimerLo;

  SOPT = 0x73;              /* Turn off the watchdog. */

  gu8RTxMode = RESET_DELAY;

  /* Add a delay to debouce the reset switch on development boards ~200ms */
  TPM1SC = 0x0D;            /*
                            * Set the Timer module to use BUSCLK as
                            * reference with Prescaler at / 32
                            */
  do {
    u8TimerHi = TPM1CNTH;   /* Get value of timer register (hi byte) */
    u8TimerLo = TPM1CNTL;   /* Get value of timer register (lo byte) */
```

```
} while (u8TimerLo <= 0x80);/*
                * Poll for TIMER LO to be greater than
                * 0x80 at 4MHz/32
                */
TPM1SC = 0x00;          /* Return to reset values */

gu8RTxMode = SYSTEM_RESET_MODE;
GPIOInit();
SPIInit();
IRQInit();              /* Turn on the IRQ pin. */
gu8RTxMode = MC13192_RESET_MODE;
PTDD_PTDD4 = 1;         /* Take MC13192 out of reset */

while (u8AttnIrq == FALSE) {
if (IRQFLAG == 1) {     /* Check to see if IRQ is asserted */
    u16IrqReg = SPIDrvRead(0x24);   /*
                        * Clear MC13192 interrupts and
                        * check for ATTN IRQ from 13192
                        */
    u16IrqReg &= 0x400;
    if (u16IrqReg == 0) {
      u8AttnIrq = FALSE;
    }
    else {
      u8AttnIrq = TRUE;
    }
  }
}

IRQSC |= 0x04;          /* ACK the pending IRQ interrupt */
IRQPinEnable();       /* Pin Enable, IE, IRQ CLR, negative edge. */
gu8RTxMode = MC13192_CONFIG_MODE;

MC13192Init();
AppInit();
SCIInit();

MLMESetMC13192ClockRate(0);  /* Set initial Clk speed */
```

```
  /*****************************************************************
 To adjust output power call the MLME_MC13192_PA_output_adjust() with:

 MAX_POWER    (+3 to +5dBm)
 NOMINAL_POWER (0 dBm)
 MIN_POWER    ~(-16dBm)

 or somewhere custom ? (0-15, 11 (NOMINAL_POWER) being Default power)

  *****************************************************************/
  MLMEMC13192PAOutputAdjust(MAX_POWER);   //Set MAX power setting
/* MLMEMC13192PAOutputAdjust(MIN_POWER);   //Set MIN power setting */
/* MLMEMC13192PAOutputAdjust(NOMINAL_POWER);   //Set Nominal power setting */

  UseExternalClock();   /* switch clock sources from mcu to MC1319x CLKO*/

#ifdef BOOTLOADER_ENABLED
  boot_init();  /* Initialize the bootloader. */
#endif BOOTLOADER_ENABLED

#ifdef BOOTLOADER_ENABLED
  boot_call();  /* Check for user request to run bootloader. */
          /* App will not return, if Bootloader is requested. */
#endif BOOTLOADER_ENABLED

  gi8AppStatus = INITIAL_STATE;   /* Initial Mode */
  if (MLMESetChannelRequest(5) == SUCCESS) { /* Select channel here (0-15) */
        gi8AppStatus = RECEIVER_ALWAYS_ON;
  }

  /* Any Button can be pressed to be put into TX mode if none
   * are pressed then it is in RX mode
   */
  TxAccel();

}
/*************************************************************
```

```
* Function:    RX_accel
* Parameters: none
* Return:      none
*
* This is the main thread of execution when no button is pressed
* on reset.
************************************************************/

void RxAccel(void) {

 EnableInterrupts;


 /************************************************************
 * RX_accel main loop
 ************************************************************/
  for(;;) {

    switch (gi8AppStatus)
    {

      case IDLE_STATE:
        /*Switch to RECEIVER_ALWAYS_ON */
        gi8AppStatus = RECEIVER_ALWAYS_ON;
        break;

      case RECEIVER_ALWAYS_ON:
          MLMERXEnableRequest(&gsRxPacket, 0);
          LOW_POWER_WHILE();
        break;

      /* Should not get here. */
      default:
        gi8AppStatus = RECEIVER_ALWAYS_ON;
            }
  }
}
/************************************************************
```

```
*   Function:    TX_accel
*   Parameters: none
*   Return:      none
*
*   This is the main thread of execution when ANY button is pressed
*   on reset.
*****************************************************************/

void TxAccel(void)
{

 /*****************************************************************
 *   TX_accel initialization
 *****************************************************************/
 SRTISC=SRTISC&~0x07; /* Disable wake up timer. */
 SPMSC2=SPMSC2&~0x03; /* Enable deep sleep mode stop3. */
 TPM1SC = 0x0F; /* Timer divide by 128. (16uS timebase for 8MHz bus clock). */

 ATD1PE=0x06; /* enable desired ADC channels (AD1, AD2 on) */
 ATD1C=0xE1; /* set prescale to 4*/


 /*****************************************************************
 *   TX_accel main loop
 *****************************************************************/

for (;;)
{

  ATD1SC = 0x01; /* read X channel */
  while((ATD1SC & 0x80) != 0x80);
  gau8TxDataBuffer[1] = ATD1RH;

  ATD1SC = 0x02; /* read Y channel */
  while((ATD1SC & 0x80) != 0x80);
  gau8TxDataBuffer[3] = ATD1RH;

/*EnableInterrupts;
```

```
 * asm {cei}
 */

  gau8TxDataBuffer[0] = 0x78; /* send x */
  gau8TxDataBuffer[2] = 0x79; /* send y */

  gsTxPacket.u8DataLength = 4;
  /*MLMETestMode(&gsTxPacket,CONTINUOUS_TX_MOD);*/
  MCPSDataRequest(&gsTxPacket); /* transmit data */


  delay(0x00FF);

  } /* end for */


} /* end main */

/*************************************************************
*  Function:    MCPS_data_indication
*  Parameters: gsRxPacket_t
*  Return:      none
*
*  This is the callback function for when a valid packet has been
*  decoded by the radio.  The valid packet is passed to the app
*   via this MCPS_data_indication callback function.  All the data
*  resides in the gsRxPacket in this function but is also passed
*  back to the main via gsRxPacket in the main/RX_accel thread.
*  This routine is in the interrupt processing call stack.  It
*  is not recommended to call other radio functions here.
*************************************************************/

void MCPSDataIndication(tRxPacket *gsRxPacket)
{

  /*
   * Place your code here to handle a mac layer data indication.
   * RX packet is in the global structure
```

```
   * gsRxPacket.dataLength and gsRxPacket.data
   */

  if (gsRxPacket->u8Status == SUCCESS)
  {

    /* Good Packet Received Check for proper x?y?z? data format */
    if ((gsRxPacket->pu8Data[0] == 'x') &&
      (gsRxPacket->pu8Data[2] == 'y'))

    {

        SCITransmitArray(&gsRxPacket->pu8Data[0], gsRxPacket->u8DataLength);
    }
  }
}

void MLMEMC13192ResetIndication (void)
{
/* Not implemented. */
}
/*************************************************************
*  Function:    AppInit
*  Parameters: none
*  Return:      none
*
*  Sets up the initial hardware initialization for the app.
*************************************************************/

void AppInit(void)
{

 /* Initialize the packet. */
 gsTxPacket.u8DataLength = 0;   /* Initialize the gsTxPacket global */
 gsTxPacket.pu8Data = &gau8TxDataBuffer[0]; /* Set the pointer to point to the tx_buffer */

 gsRxPacket.u8MaxDataLength = 0;
 gsRxPacket.pu8Data = &gau8RxDataBuffer[0];
```

```
 gsRxPacket.u8MaxDataLength = 16;   /* Arbitrary, bigger than xXyYzZ format. */
 gsRxPacket.u8Status = 0;           /* initialize status to 0. */
}
/*****************************************************************
*  Function:    delay
*  Parameters: 16-bit delay value
*  Return:      none
*
*  Simple delay loop.
*****************************************************************/

void delay(INT16 count)
{
  INT16 i;
  for (i=0; i<count; i++);
}
```